

# Physical volcanology and geochemistry of the Carlton Rhyolite in the Slick Hills, Wichita Mountains

**Richard E. Hanson<sup>1</sup>, Barbara K. Burkholder<sup>2</sup>, R. Nowell Donovan<sup>3</sup>, Jennifer C. Dart<sup>4</sup>, Stephen J. Frazier<sup>5</sup>, David A. McCleery<sup>6</sup>, Christine M. Philips<sup>7</sup>, and Julie B. Pollard<sup>8</sup>**

<sup>1</sup>*School of Geology, Energy, and the Environment, Texas Christian University, Fort Worth, Texas 76129. r.hanson@tcu.edu. Corresponding author.*

<sup>2</sup>*St. Anthony Falls Laboratory, University of Minnesota, Minneapolis, Minnesota 55419. bkb0811@umn.edu.*

<sup>3</sup>*School of Geology, Energy, and the Environment, Texas Christian University, Fort Worth, Texas 76129. r.donovan@tcu.edu.*

<sup>4</sup>*CB&I Environmental & Infrastructure, Inc., Dallas, Texas 75234. jennifer.dart@CBI.com.*

<sup>5</sup>*Freeport-McMoran Oil and Gas, Houston, Texas 77002. stephen\_frazier@fmi.com.*

<sup>6</sup>*School of Geology, Energy, and the Environment, Texas Christian University, Fort Worth, Texas 76129. d.mcleery@tcu.edu.*

<sup>7</sup>*32268 Brincrest Drive, Farmers Branch, Texas 75234. cmphilips@gmail.com.*

<sup>8</sup>*Watauga Middle School, Watauga, Texas 76148. julie.pollard@birdvilleschools.net.*

## INTRODUCTION

The Slick Hills are the exposed parts of a structurally complex block that is bordered by faults of the Frontal Fault Zone, which defines the tectonic boundary between the main igneous core of the Wichita Uplift to the south and the deep Anadarko Basin to the north (Harlton, 1963; Ham et al., 1964; McConnell, 1989; Donovan, 1982, 1995). Important outcrops of the Carlton Rhyolite Group are exposed in the Slick Hills along with unconformably overlying Upper Cambrian to Ordovician strata of the Timbered Hills and Arbuckle Groups. Deformation of the well-bedded sedimentary package in places has resulted in a complicated array of folds and faults (Donovan, 1986; McConnell, 1989), but the rhyolites are less strongly deformed. They form a discontinuous series of outcrops extending in a southeast-northwest direction from the Blue Creek Canyon area to Zodletone Mountain (Figures 1 and 2). The structural domain containing the rhyolites is bound on the southwest by the Blue Creek Canyon Fault, which is an oblique, west-vergent reverse fault with a left-lateral component of slip that splays off the major Meers Fault to the south (Fig. 1; McConnell, 1989; Donovan, 1982, 1995). The Blue Creek Canyon Fault is only exposed in Blue Creek Canyon, where it deforms parts of the Carlton Rhyolite in that area (McCall, 1994).

We have mapped most of the rhyolite outcrops in the Slick Hills. Exceptions include a few small relatively small exposures of rhyolite in the northwest part of the area

shown in Figure 2 where we have been unable to obtain permission from the property owners to gain access. The laterally most extensive outcrops occur in the Blue Creek Canyon area. The other rhyolite exposures farther northwest form a series of small knobs and more prominent hills rising above the prairie. The thickest exposed stratigraphic sequence of rhyolites occurs in the Bally Mountain area and is  $\geq 2$  km thick. Rhyolites are also exposed on smaller hills a short distance along strike northwest of Bally Mountain, but we interpret those rocks to be separated from the rhyolites on Bally Mountain by a fault (Fig. 2). Additional rhyolite outcrops occur in the Zodletone Mountain area, which represents the northernmost exposure of igneous rocks related to the Wichita Province.

The unconformity between the rhyolites and the overlying lower Paleozoic sedimentary strata is well exposed in the Blue Creek Canyon and Bally Mountain areas. The actual contact is covered at Zodletone Mountain, but the stratigraphically highest rhyolite outcrops there are only a short distance from exposures of the overlying sedimentary section. Where the unconformity can be directly observed, fluvial deposits at the base of the Upper Cambrian Reagan Sandstone in the lower part of the Timbered Hills Group generally rest directly on an erosional surface carved into the rhyolites. The fluvial deposits are succeeded by Upper Cambrian-Ordovician shallow-marine clastic and carbonate rocks in the upper part of the Timbered Hills Group and overlying Arbuckle Group (Donovan, 1986). Paleorelief on the unconformity surface is markedly irregular in places,

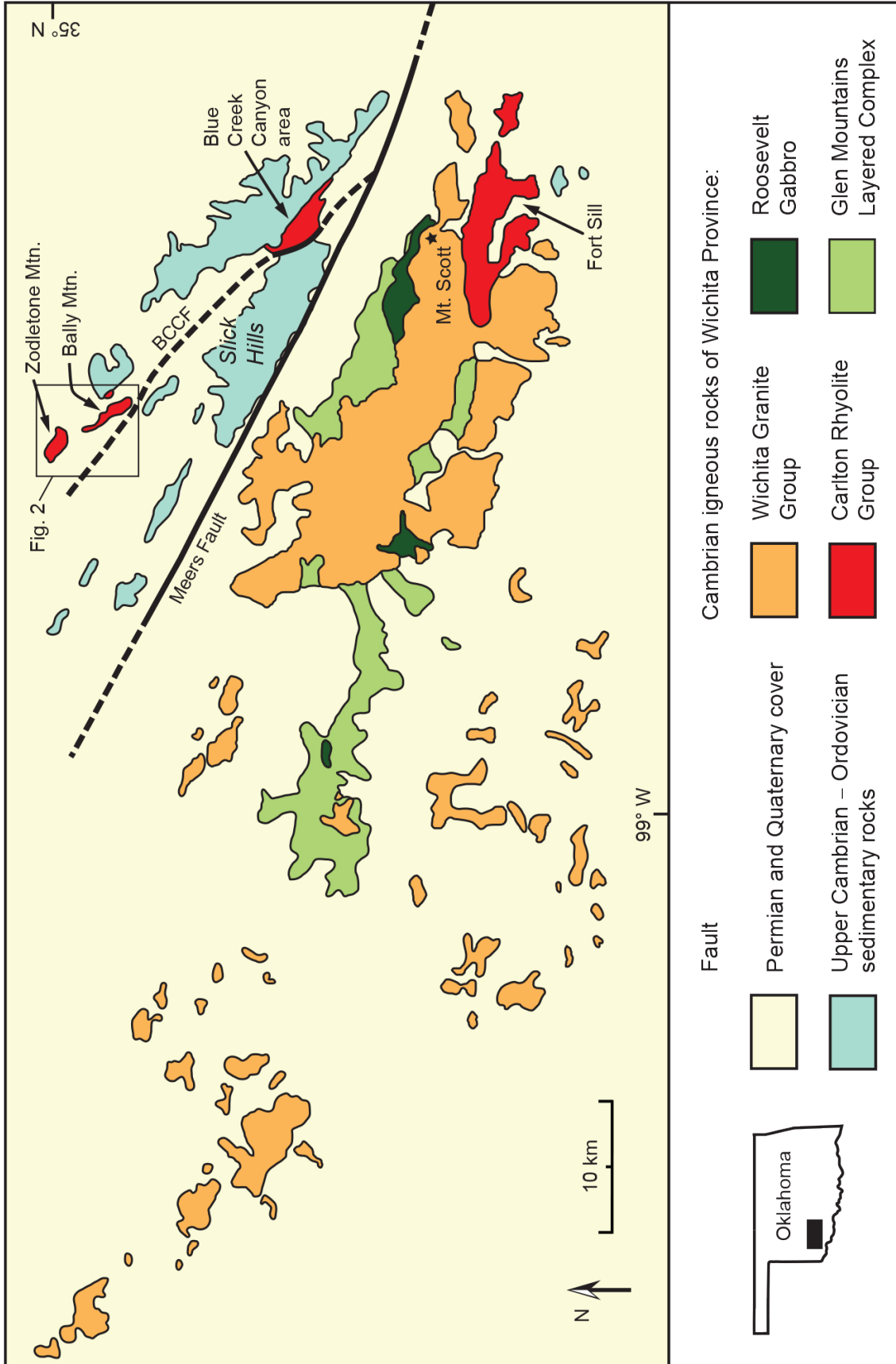


Figure 1. Simplified geological map of the Wichita Mountains, modified from Powell et al. (1980) and Donovan (1995). Area of Figure 2 is indicated. *BCCF*: Blue Creek Canyon Fault.

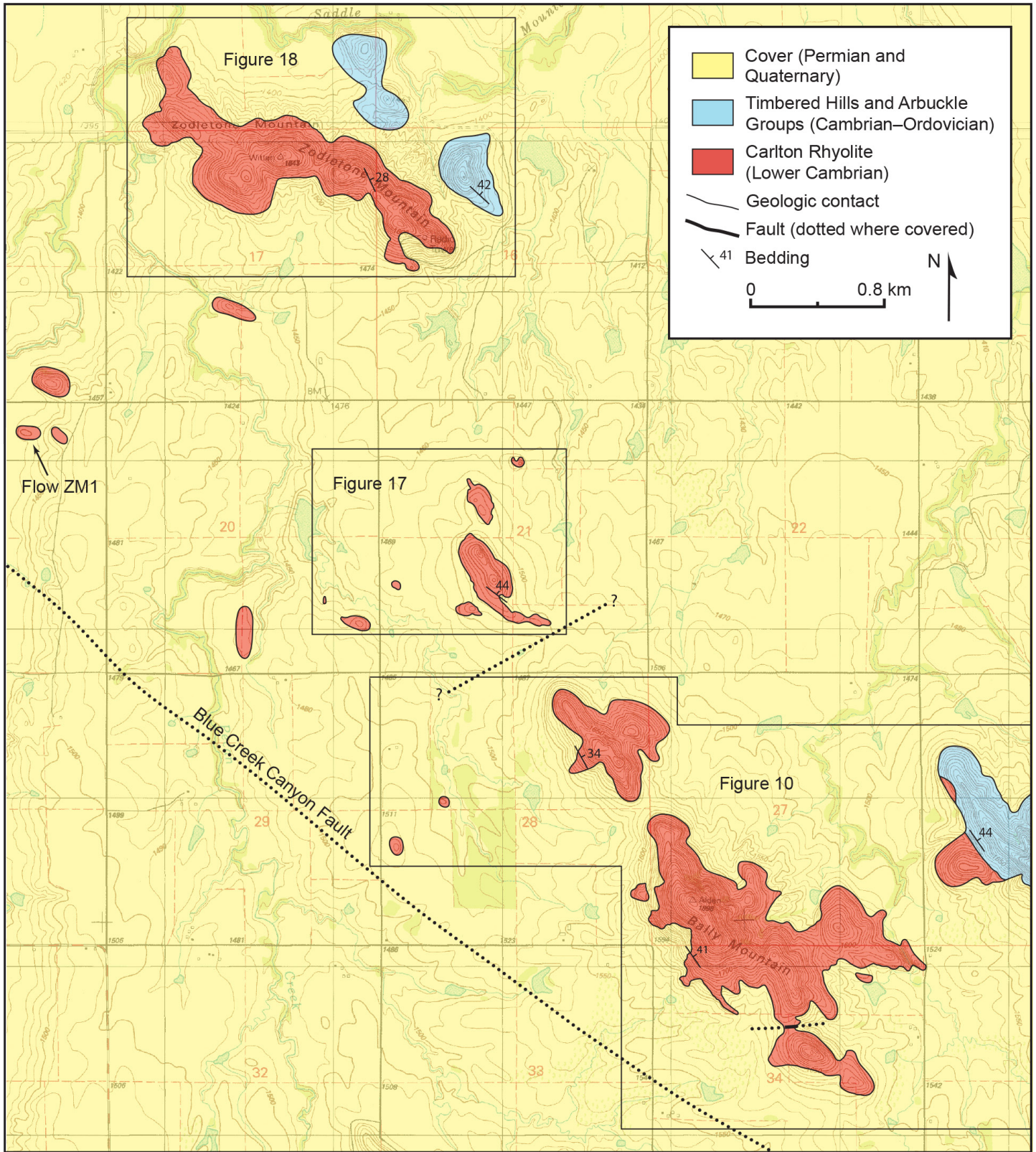


Figure 2. Geologic map of part of the Slick Hills, based on Miller and Stanley (2004), Stanley and Miller (2005), and our mapping. Locations of more detailed maps appearing in later figures in this paper are outlined.

and paleohills of rhyolite rise in some cases into the lower Arbuckle Group (Donovan et al., 1988a; Donovan and Bucheit, 2000).

In the Bally Mountain and Blue Creek Canyon areas, flow banding or flow parting that is assumed to be parallel to flow bases and tops shows an angular discordance of  $\sim 5^\circ$  with the basal lower Paleozoic strata (Donovan, 1986; Donovan et al., 1988a). The boundaries between the three stratigraphically highest rhyolite flows in the Blue Creek Canyon area are also truncated at the unconformity (Philips, 2002). Although the angular discordance is slight, on a regional scale a significant thickness of rhyolite may have been removed by erosion along this beveled contact prior to or during Late Cambrian marine transgression across the region.

Diabase intrusions, which represent the last phase of igneous activity in the Southern Oklahoma Aulacogen, have been mapped in a number of the rhyolite outcrops (e.g., Hanson and Philips, Stop 4, this guidebook) but are typically poorly exposed. The diabases weather much more readily than the rhyolites, and there are probably many more diabase intrusions in the area than are currently recognized. They occur as dikes and sills as well as gently inclined sheets that cut layering in the volcanic succession at a low angle. A related intrusion is the Kimbell Gabbro, which is somewhat larger and coarser grained than the diabases and forms a body  $\geq 160$  m across that cuts rhyolite in Blue Creek Canyon (DeGroat et al., 1995).

## GENERAL VOLCANOLOGICAL FEATURES

Rhyolites in the Slick Hills show a consistent vertical zonation of textures and structures related to emplacement and cooling, as described below, which allows contacts between flows to be recognized and mapped in this ancient volcanic field even where outcrop is fairly poor. We have identified 29 flows in the various rhyolite outcrop areas in the Slick Hills. It has not been possible to correlate flows between the main outcrop areas, at least partly because of structural complications. The flows are numbered from the base to the top in each of these areas, which are indicated by prefixes to the flow numbers, with “BC” for the Blue Creek Canyon area, “BM” for Bally Mountain, “NBM” for hills northwest of that mountain, and “ZM” for Zodletone Mountain. Characteristics of the individual flows are given in the appendix.

Contacts between different flows are generally covered. In a few cases where outcrop is good, one flow can be seen to rest directly on the underlying one. In a number of other cases, interbeds of tuffaceous mudstone or crys-

tal-vitric tuff  $< 1$  m thick occur between flows and contain well-preserved tricusate bubble-wall shards and ash-sized pumice clasts replaced by silica (e.g., fig. 12 in Hanson and Eschberger, this guidebook). Some of the tuff interbeds mantle surface irregularities on the underlying flow and are interpreted to record direct fallout of ash from the atmosphere. In other cases, they show small-scale cross-lamination, indicating slight reworking of ash-fall deposits.

Representative modal analyses for the ZM and BC flows are given in Table 1 and show that alkali feldspar and plagioclase combined make up  $\sim 6$  to 24% of the total rock volume. Quartz phenocrysts are absent in some flows or occur only in small amounts. Modal analyses are not yet available for the BM and NBM flows, but visual estimates indicate that phenocryst contents in those rhyolites are generally similar to the values shown in Table 1. Quartz phenocrysts, however, are somewhat more abundant in the BM and NBM flows where they make up as much as 3% of the total rock in some flows and are present in amounts of  $\sim 5$  to 10% in a few flows.

### Vertical Zones within Individual Flows

A schematic section of an idealized Carlton Rhyolite flow is shown in Figure 3, although it should be pointed out that only some of the flows contain the complete sequence of zones depicted there. However, the zones in almost all cases occur in the same vertical sequence wherever they are present. The zones tend to be best defined in the thicker flows. As discussed in Hanson and Eschberger (this guidebook), the regular development of these zones implies that most of the flows were emplaced as single, relatively thick sheets that underwent slow, uniform cooling after emplacement. This, in turn, is consistent with the idea that the outcrops in the Slick Hills are, at least in some cases, remnants of laterally extensive flows similar to those documented in many other A-type felsic volcanic provinces (Hanson and Eschberger, this guidebook).

### Chilled Glassy Margins

The rapidly chilled upper and lower margins of the flows are defined by zones of altered and devitrified glass. Perlitic texture is widespread in these marginal zones (Fig. 4A), recording hydration of the glass after emplacement. Devitrification of the hydrated glass after the flows cooled to ambient temperatures has produced an extremely fine grained mosaic of intergrown quartz and feldspar in which individual mineral phases are only partly resolvable at highest magnification. The unstable glass also experienced

TABLE 1. MODAL ANALYSES FOR RHYOLITES IN BLUE CREEK CANYON AND ZODLETONE AREAS

	Blue Creek Canyon						Zodletone Mountain		
	Flow BC2	Flow BC3	Flow BC4	Flow BC5	Flow BC6	Flow BC7	Flow ZM3	Flow ZM4	Flow ZM5
Feldspar	16.5 %	17.9 %	20.5 %	9.2 %	6.0 %	12.2 %	23.6 %	21.6 %	17.0 %
Quartz							1.8 %		
Mafics	7.2 %	7.4 %	6.9 %	1.9 %	2.4 %	0.8 %	6.1 %	6.4 %	7.4 %
Groundmass	76.3%	74.7 %	72.6 %	88.9 %	91.6 %	87 %	68.5 %	72.0 %	75.6%

Modal analyses on cut slabs; 500 points counted. Mafics include titanomagnetite and pseudomorphs of mafic silicates.

significant alteration, resulting in replacement of much of it by green clay, which gives these zones a dark-gray, dark-green, or black color in hand sample. In some cases, the glassy zones exhibit a delicate flow lamination, but in other cases they appear to be massive in hand sample, possibly because formation of perlitic cracks and subsequent alteration have obscured any primary flow-related features.

Small, irregular vesicles aligned in the direction of flow and ranging from <1 mm to ~1 cm across occur in variable amounts in the glassy margins. They are partly to completely filled with silica or green clay. In a few cases, the vesicles become so abundant that the rhyolite is pumiceous (e.g., flows BC3 and BM8, appendix).

### ***Lithophysal Zones***

Lithophysae are abundant within the inner parts of the glassy margins in a number of the flows (Figs. 4B and 4C). Lithophysae are spherulites or other types of devitrification domains in felsic lavas and densely welded ignimbrites that contain internal cavities and form either from still molten lava or during high-temperature devitrification (McArthur et al., 1998; Breitreuz, 2013). In the Carlton Rhyolite, the lithophysae generally consist of spherulitic intergrowths extending from a central gas cavity out into what was originally glass. The cavities have cusped outlines (Fig. 4C), reflecting their formation near the glass-transition temperature during cooling, with the cavities growing partly by ductile expansion and partly by tearing of the stiffening glass. Cavities of this type probably form from volume contraction of the lava during cooling coupled with exsolution of gas (Breitreuz, 2013).

Lithophysae in the Carlton Rhyolite are typically  $\leq 5$  cm across, but in flow BC6 they are as much as 30 cm across (Bigger and Hanson, 1992). They developed after

flow ceased because in all cases they truncate flow banding in the adjacent, originally glassy lava. Because the lithophysae are more resistant to weathering than the altered glass, they commonly collect as loose spheres on outcrop surfaces. The lithophysal zones tend to be best developed near flow tops. The restricted occurrence of the lithophysae only near the upper and lower flow margins suggests that their formation required a delicate balance between cooling rate and gas release.

The gas cavities at the centers of the lithophysae in the Carlton Rhyolite are commonly lined by chalcedony and/or fine-grained, drusy quartz crystals, presumably deposited from migrating groundwater long after volcanism ceased. In lithophysae described from Cenozoic felsic volcanic rocks, the gas cavities may be lined with a variety of minerals precipitated from high-temperature gases concentrated in the cavities, including cristobalite and tridymite, the high-T/low-P polymorphs of silica (e.g., Ross and Smith, 1961; Swanson et al., 1989). Bigger and Hanson (1992) reported paramorphs of quartz after cristobalite and tridymite in the gas cavities at the center of the large lithophysae in flow BC6, and we have subsequently observed similar quartz paramorphs after cristobalite in lithophysae in the northwest Bally Mountain area.

### ***Flow Banding and Flow Breccia***

Flow banding in some cases begins at the base and top of the flows, but in other cases it begins to appear inward from an interval of apparently featureless glass. On the outcrop scale, the flow banding is defined by layers as much as a few centimeters thick of dark-colored, originally glassy material alternating with layers of holocrystalline, pink-gray to orange-gray rhyolite (Figs. 5A and 5B). A delicate flow lamination extending down to the thin-section scale is also

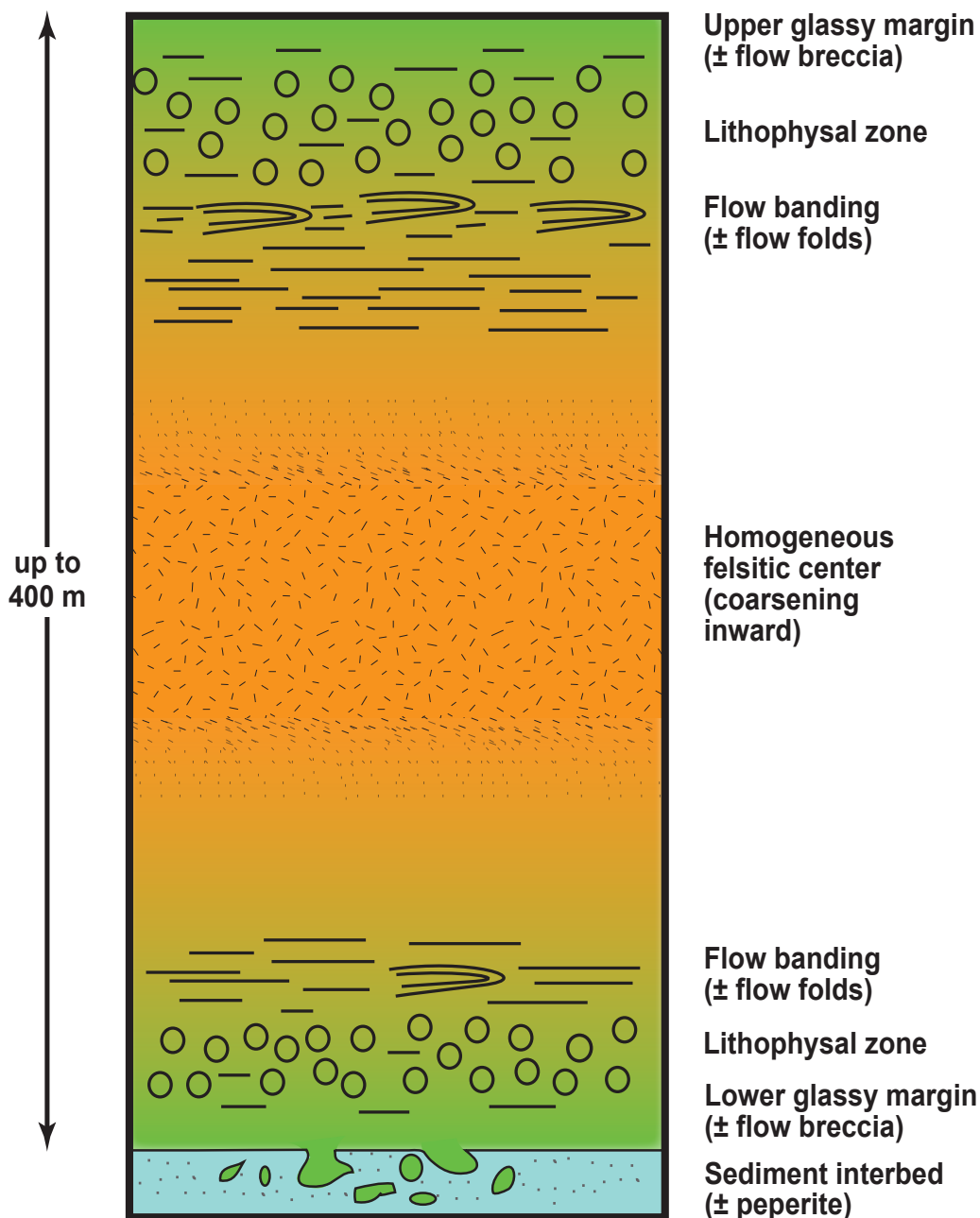


**Figure 3. Vertical zonation within an idealized Carlton Rhyolite flow.**

present in many cases, particularly in the more glassy layers (Figs. 5C and 5D). Perlitic texture is well preserved in many of the originally glassy layers but terminates at the boundary with adjacent holocrystalline layers, which typically show well-developed spherulitic texture. We interpret these textural differences to indicate that the holocrystalline layers underwent high-temperature devitrification during initial cooling of the flows after emplacement. The remaining layers stayed glassy and experienced hydration, alteration, and long-term

low-temperature devitrification. Similar types of flow banding occur in younger, better preserved rhyolite lavas. One explanation for the development of the banding, which may be applicable in the present case, is that the layers that underwent early, high-T devitrification were originally richer in dissolved volatiles. This would have speeded up devitrification rates in those layers, resulting in complete devitrification at an early stage of cooling (Seaman et al., 2009).

The flow banding in many cases is parallel or subparallel to the lower and upper contacts of the flows, but in other cases it shows a wide range in orientation due to folding of the banding during flow emplacement. These flow folds have wavelengths of several meters down to the submillimeter scale (Figs. 5C, 5D, 6A, and 6B). They range from gentle, open warps to highly attenuated isoclinal folds, and complex zones of refolding occur in places. Flow lineation occurs on the surfaces of some flow bands or laminae (Fig. 6C) and presumably was produced by shear between surfaces of stiffening lava during flow emplacement. Where the flow folds can be observed in three dimensions, the flow lineation is in many cases parallel to the fold axes, implying that these folds have sheath-like geometries resulting from rotation

of fold hinges into the direction of transport within zones of intense ductile shearing during flow of the lava (e.g., Branney et al., 2004).

In some cases along the upper and lower flow margins, flow-banded lava grades into zones of flow breccia as much as 70 m thick (Fig. 6D). Early stages in breccia formation involve incipient breakup of flow bands, and these areas pass progressively into zones of chaotic breccia as clasts show increased degrees of fragmentation and rotation relative to each other. In some flow-breccia zones,

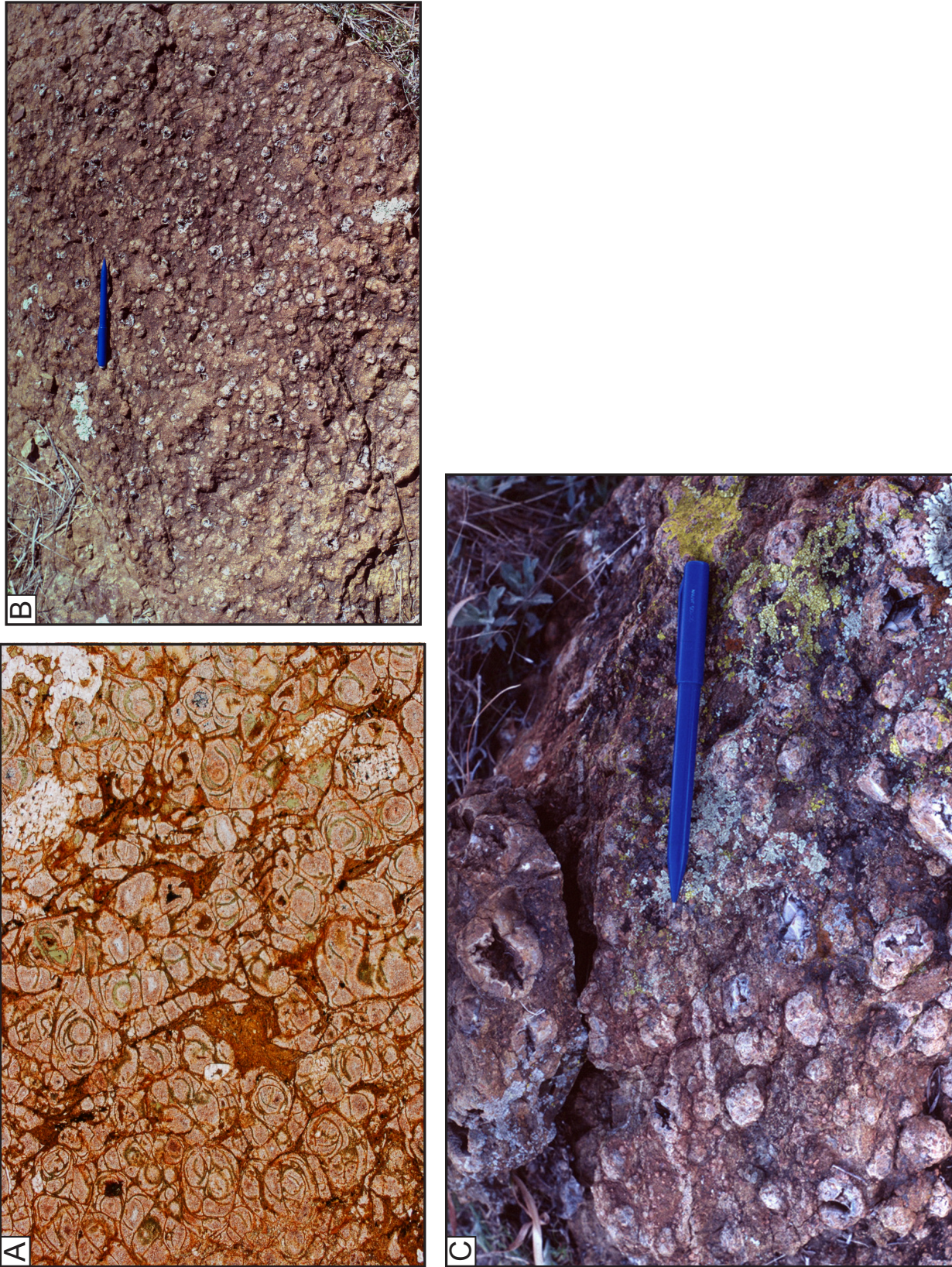


Figure 4. (A) Photomicrograph showing perlitic texture in chilled margin at top of flow BC4 (see text for explanation of flow names). Two partly resorbed plagioclase phenocrysts are visible in upper right. Plane-polarized light; field of view ~5 mm across. (B) Zone rich in small lithophysae in lower part of flow BC2. Cavities within lithophysae are lined by white quartz. Pencil for scale is 14 cm long. (C) Lithophysae near top of flow BM5. Central cavities show typical cusped shapes and are lined by fine-grained drusy quartz and agate. Flow banding is visible to left of pencil tip.

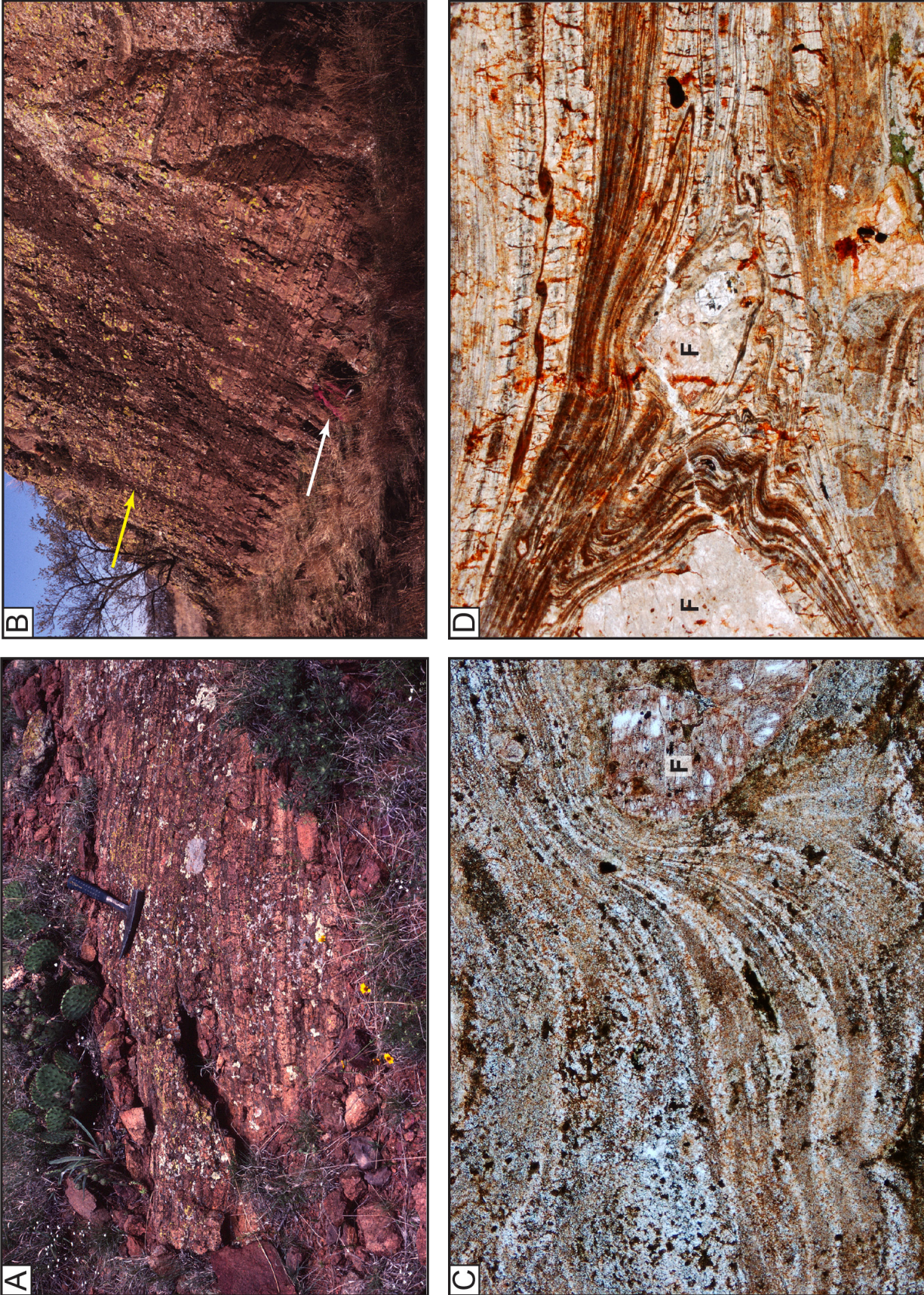


Figure 5. (A) Flow banding in lower part of flow BM9. (B) Flow banding at the base of flow BM7. The banding is parallel to the flow base and is crossed at right angles by columnar joints (one example is indicated by yellow arrow). Daypack (white arrow) for scale. (C) Photomicrograph showing flow lamination wrapping around a feldspar phenocryst (*F*) near base of flow ZM5. Plane-polarized light; field of view ~2.5 mm across. (D) Photomicrograph showing flow lamination deformed by microscopic isoclinal flow folds near top of flow BC5. *F*: feldspar phenocrysts. Plane-polarized light; field of view ~2.5 mm across.

rafts of flow-banded lava as much as several meters long are surrounded on all sides by breccia.

### ***Flow Interiors***

Zones of flow banding grade inward into homogeneous flow interiors as the banding becomes less distinct. The flow interiors consist of nonvesicular, pink-gray to orange-gray felsitic rhyolite, which is the dominant rock type in the thicker flows. In thin section an early generation of small, dispersed spherulites is visible in the felsitic rhyolite, but thin, elongate tridymite needles (now inverted to quartz) of the type described in Hanson and Eschberger (this guidebook) generally dominate the texture. Very fine grained, more or less subequant quartz and feldspar occupy interstices between the tridymite crystals. Some of the tridymite needles extend radially from the early spherulites, and others appear to be randomly oriented (fig. 7 in Hanson and Eschberger, this guidebook); they show no evidence of alignment in the direction of flow. They are coarsest in flow centers and show a gradational decrease in size towards the upper and lower flow margins, consistent with other evidence that individual rhyolite flows underwent uniform cooling following emplacement.

### ***Topographic Expression of Flow Zonation***

The vertical zonation within flows leads to a characteristic topographic expression, which is a great help in tracing flows laterally. Felsitic flow interiors are significantly more resistant to weathering and erosion than the glassy margins and tend to form linear ridges. As a general rule, the highest topographic features in the rhyolite outcrop areas within the Slick Hills are underlain by the felsitic interiors of flows. The prominent peak of Bally Mountain provides a good example (Fig. 7A). In contrast, the glassy chilled margins form poor exposures in topographically low, grassy areas and in many cases are recognized primarily by the appearance of small pieces of float derived from the dark-colored, originally glassy rock.

### ***Peperite at the Base of Flows***

Peperite is developed along the bases of many of the rhyolite flows where they overlie interbeds of tuffaceous mudstone or tuff. Peperite refers to a rock developed where magma (in this case lava) interacts with generally wet, unlithified sediment. Quenching and disruption of the magma ensues, along with intermixing between quenched igneous debris and the weak, incoherent sediment (Skilling et al., 2002). Peperites in the Carlton Rhyolite in most cases are limited to zones <1 m thick at the base of flows. Textures

shown by the peperites are best exemplified in an extensive zone of peperite that occurs beneath flow BM3 and is described in more detail below.

### ***Joints Related to Flow Emplacement and Cooling***

Most rhyolite flows exposed in the Slick Hills exhibit several different types of jointing that originated during flow emplacement and cooling from magmatic temperatures. Tectonic joints related to late Paleozoic deformation and, possibly, to Early Cambrian rifting are also present but will not be discussed here.

#### ***Columnar Joints***

Columnar joints are variably developed in many of the flows and formed due to volume reduction during solidification of the molten lava. The columns are typically 1.0-1.5 m across (Figs. 7B and 7C) and in some cases exhibit regular hexagonal shapes, with 120° angles between column faces. Many of the columns are less well developed, although angles between at least some of their faces approach 120°. The columns are generally oriented perpendicular to the bases and tops of individual flows and in some cases extend all the way to the bases (Fig. 5B).

#### ***Sheeting Joints***

Sheeting joints are a less well understood type of joints that is common in the Carlton Rhyolite, both in the Slick Hills and elsewhere in rhyolite outcrops in the Wichita and Arbuckle Mountains (Eschberger et al., this guidebook; Finegan and Hanson, this guidebook). Bonnicksen and Kauffman (1987) used the term sheeting joints to refer to closely spaced, subparallel joints found within the devitrified parts of large-volume Miocene A-type rhyolite lava flows in the Snake River Plain, Idaho. The sheeting joints are absent in the glassy chilled margins of the flows, and Bonnicksen and Kauffman (1987) considered the joints to have developed due to the volume change occurring during devitrification of glass.

Sheeting joints in the Carlton Rhyolite are generally spaced a few centimeters apart, but in places the spacing decreases to ~0.5 cm. Although individual joints are subparallel to adjacent joints for part of their length, they typically show wedge-shaped terminations against the adjacent joints. The sheeting joints cut across columnar joints in the flows (Fig. 7C) and, where most strongly developed, may largely obscure the columns. In the simplest cases, a single set of sheeting joints is present subparallel to flow bases or tops. In other cases, the sheeting joints are curvilinear (Figs.

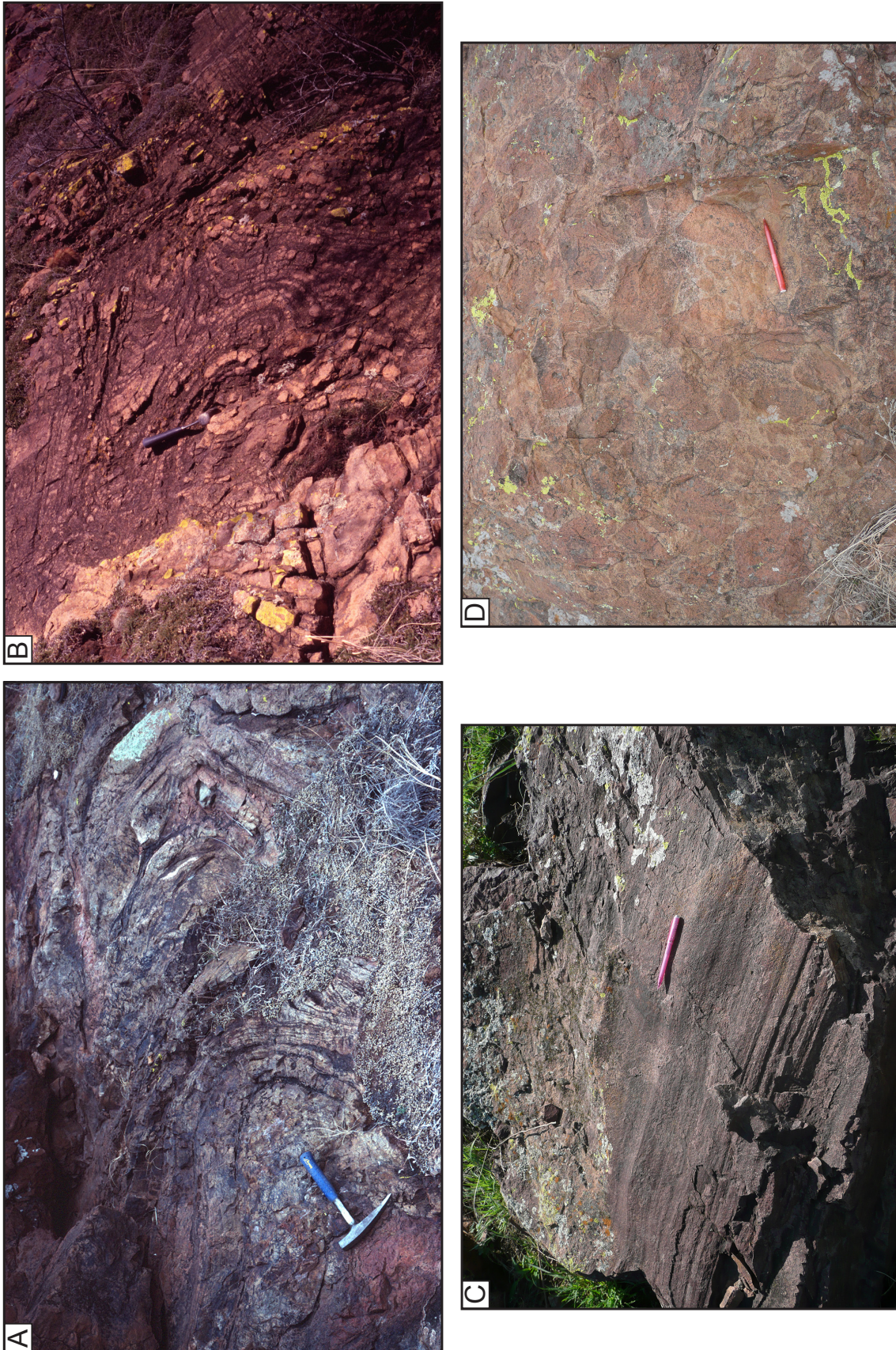


Figure 6. (A) Flow fold in lower part of flow BC6. (B) Complex flow folding in lower part of flow BM7. (C) Flow lineation on surface of flow band in lower part of flow BM1. (D) Flow breccia at the base of flow NBM7. Light-colored interstitial material is finely comminuted debris derived from abrasion or breakup of larger clasts.

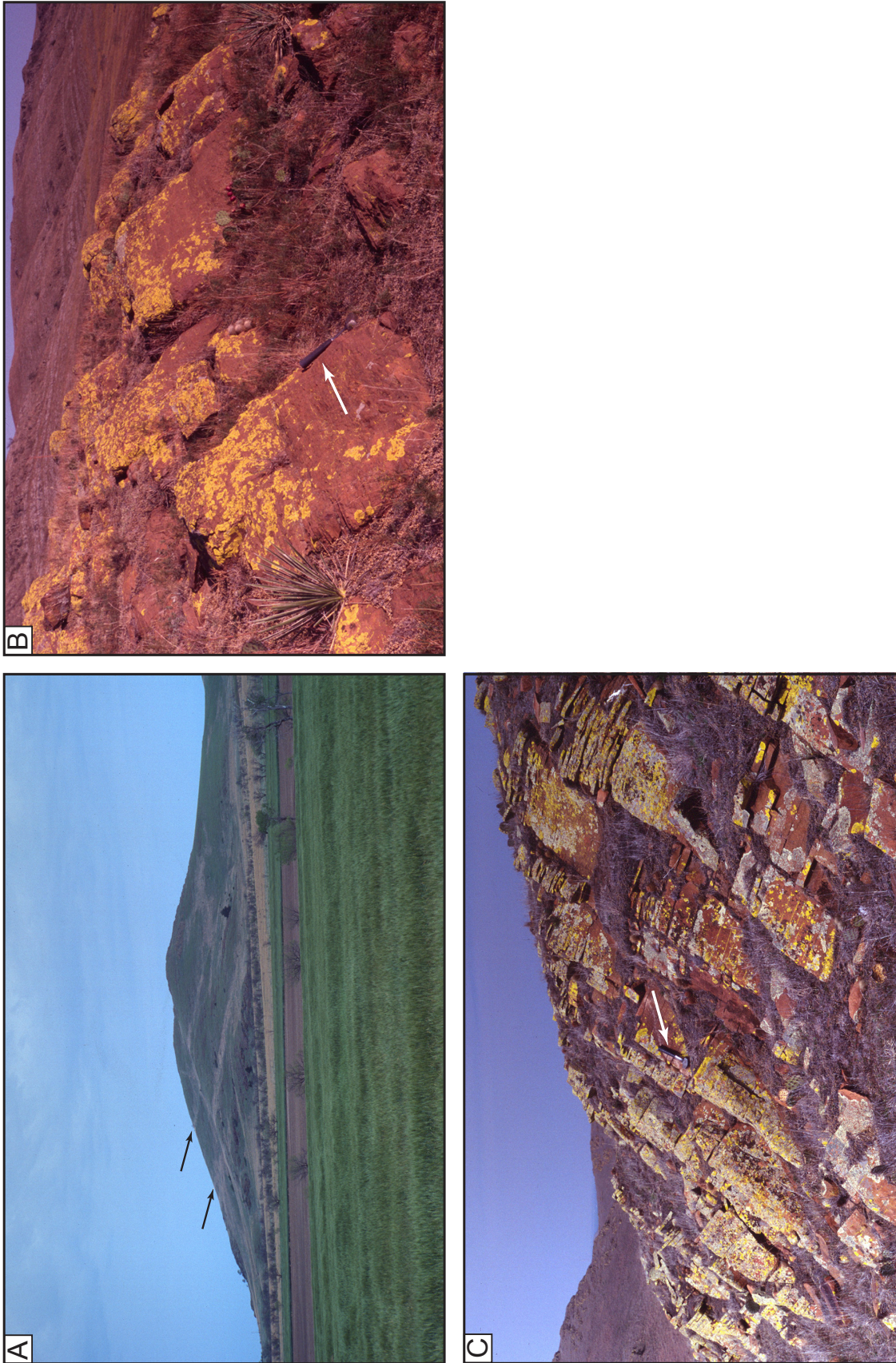


Figure 7. (A) View looking north at Bally Mountain. Arrows point to prominent benches believed to represent intrusive diabase sheets cutting flow BM3 (Figs. 10 and 11). Outcrops of flow BM2 are visible near base of mountain beneath the lower bench. The rest of the rhyolite visible in this view is within the lower and middle parts of flow BM3. (B) Columnar joints in lower part of flow BM9. Hammer (arrow) rests on a column plunging to the right. Stratigraphically overlying Upper Cambrian and Ordovician sedimentary strata are visible on steep hillside in background. (C) Columnar joints in lower part of flow BM3 crossed at right angles by sheeting joints. Hammer (arrow) rests on a column plunging to the left.

8A and 8B) and their attitude may be highly variable, ranging from subhorizontal to subvertical over short distances. As in the Miocene examples described by Bonnicksen and Kauffman (1987), the sheeting joints do not extend into the chilled upper and lower margins of the flows in the Carlton Rhyolite. One of us (Hanson) has visited some of the flows in the Snake River Plain described by Bonnicksen and Kauffman (1987), and the sheeting joints in the Miocene flows are virtually identical to those in the Carlton Rhyolite. We therefore interpret this style of jointing in the Carlton Rhyolite to be the result of volume decrease during devitrification. Absence of the jointing in the chilled, originally glassy margins of the flows indicates that it formed during primary devitrification associated with initial cooling from magmatic temperatures, rather than slow, long-term devitrification at ambient temperatures.

### **Flow Parting**

We use the term flow parting to refer to parallel joints that are more closely spaced than typical sheeting joints and are more regularly developed. In flow parting, the joints are typically spaced ~0.5 to 2 cm apart and may impart a flaggy appearance to rhyolite outcrops. Unlike flow banding, the rhyolite between individual joint surfaces in flow parting shows no observable change in color or texture. Flow parting in some cases occurs together with true flow banding, where it follows individual flow bands, but it also persists farther into the flow interiors than the flow banding. Its mode of formation is uncertain, but it may represent discrete planes of laminar shear that developed late in the motion of the lava as it began to stiffen. Unlike sheeting joints, flow parting in almost all cases is developed parallel to flow bases and tops. Flow parting appears to grade into more widely spaced sheeting joints in some cases, and the two types of jointing may be closely related.

## **DESCRIPTIONS OF INDIVIDUAL OUTCROP AREAS**

### **Blue Creek Canyon**

Rhyolite exposed in the Blue Creek Canyon area (Fig. 9) is affected by several faults described by Hanson and Philips (Stop 4, this guidebook). Seven flows have been identified in the area and range from 150 to 230 m thick (Philips, 2002); the total exposed stratigraphic thickness of rhyolite is ~1 km. The map pattern indicates that the flows are tabular, and they can be traced for as much as 3.8 km along strike before being truncated by faults or the

unconformity with the overlying lower Paleozoic sedimentary strata. Areas where we are unsure of the stratigraphic position of the rhyolites are shown as undivided rhyolite in Figure 9. In the vicinity of the Blue Creek Canyon Fault, the undivided rhyolite shows strong brittle deformation that has obscured some of the primary volcanic features. The more extensive mass of undivided rhyolite east of the Ketch Creek Fault (Fig. 9) shows pervasive flow banding, but we were unable to find evidence of a flow boundary in that area. It may represent a separate flow unrelated to the flows mapped to the west.

Coherent interbeds of vitric tuff as much as 30 cm thick are exposed discontinuously along contacts between four of the Blue Creek Canyon flows (Fig. 9). In places the interbeds grade laterally into thin zones of peperite where they were thoroughly disrupted as the overriding lava quenched against and mixed with the unconsolidated ash. Although not present as intact layers, tuffaceous mudstone and fine-grained rhyolitic volcanoclastic sandstone also occur as the sediment host in some of the peperites.

Only one hypabyssal rhyolite body intruding the extrusive rhyolites has been found in the Slick Hills, in contrast to some other parts of the Carlton Rhyolite Group (Eschberger et al., paper, this guidebook). The intrusion occurs in the Blue Creek Canyon area in the lower part of flow BC6. It is  $\leq 20$  m thick, making it too small to show accurately in Figure 9, and forms a resistant layer with columnar jointing perpendicular to its upper and lower contacts. We interpret the intrusion to be a sill, although its lateral extent is unclear because of poor exposure. It has a similar phenocryst content to flow BC6 but a markedly different chemical composition, as shown in the section on geochemistry below.

### **Bally Mountain**

Ham et al. (1964) first studied the rhyolite outcrops on Bally Mountain (Fig. 10) in detail and published a measured section across the main outcrop area, starting at the base of the lowest rhyolite outcrops on the southwest side of the mountain. Those workers measured a total thickness of rhyolite of ~1.1 km extending to the unconformity with the overlying lower Paleozoic sedimentary rocks to the northeast. They recognized 18 separate rhyolite intervals in the succession based on outcrop characteristics and variations in textures and flow structures in the rhyolites. We interpret many of these intervals to represent distinct zones within flows of the type depicted in Figure 3, which allows recognition of nine separate flows in the



**Figure 8. (A) Outcrop in flow BM3 near top of Bally Mountain showing sheeting joints with varying attitudes. Note curviplanar joints in lower center above grass. (B) Sheeting joints in same general area showing wedge-shaped terminations between joints in foreground. Hammer (arrow) rests on curviplanar joints in background.**

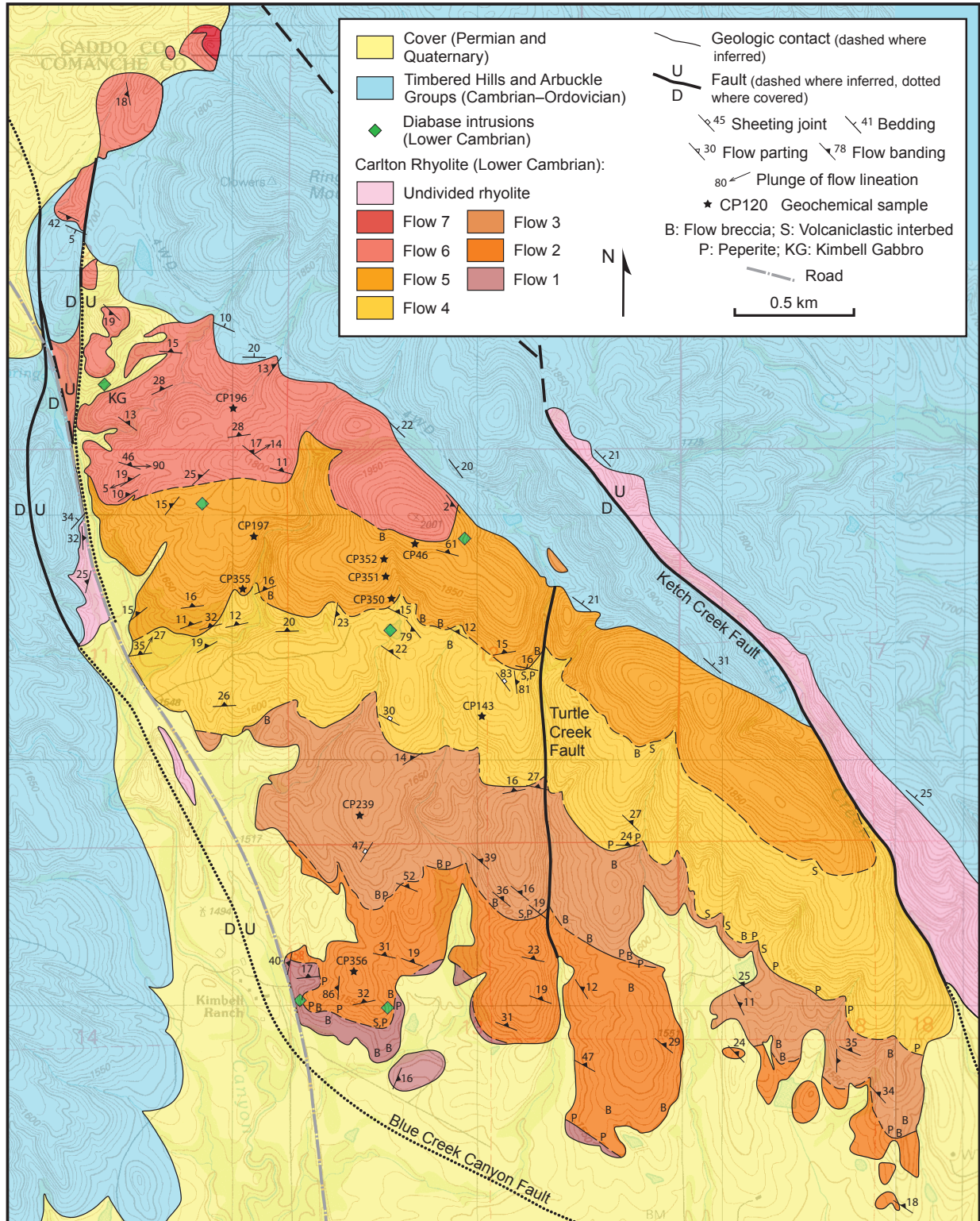


Figure 9. Geologic map of the Carlton Rhyolite in the Blue Creek Canyon area, from Philips (2002); faults and Upper Cambrian-Ordovician sedimentary rocks are from Donovan et al. (1986) and McCall (1994).

Bally Mountain area (Fig. 10). Also, we consider isolated outcrops in small hills west of Bally Mountain as part of the same overall succession, which increases the total stratigraphic thickness of the rhyolite present in the area to ~2 km. This represents the maximum stratigraphic thickness of rhyolite so far documented in the Carlton Rhyolite Group. The stratigraphically lowest and highest flows have yielded U-Pb zircon dates of ~532 Ma (Hanson et al., 2009), and locations of the dated samples are indicated in Figure 10.

Relatively thick, well-preserved sequences of bedded volcanoclastic rock occur in two parts of the Bally Mountain succession and will be described below. Four parallel, grass-covered benches on Bally Mountain were noted by Ham et al. (1964), who considered the benches to be concordant with the rhyolite flows and suggested that they are underlain by diabase or basalt. Two of the benches occur on the southwest side of Bally Mountain and are obvious even from a distance (Fig. 7A). Our mapping shows them to dip more gently to the northeast than the rhyolite flows exposed in the area, and the lower bench cuts partly across the stratigraphy defined by bedded volcanoclastic rocks and an underlying zone of peperite (Figs. 10 and 11). In the northern part of the area shown in Figure 11, the bench occurs beneath the bedded volcanoclastic sequence. Farther to the southeast, the bench occurs at the top of the volcanoclastic sequence, between it and the base of flow BM3. We interpret the benches to represent diabase intrusive sheets that transgress the layering in the volcanic succession at a low angle. A poorly exposed diabase sill intrudes bedded volcanoclastic rock on the southwest side of the smaller hill northwest of Bally Mountain (Fig. 10), but it is uncertain whether this sill connects directly with one of the benches on Bally Mountain.

The high points on the mountain are held up by the interior felsitic zone of a single flow 370 m thick (flow BM3), which represents the thickest flow known in the Wichita Mountains and one of the thickest flows that has so far been documented in the entire Carlton Rhyolite Group. The best examples of sheeting joints that we have found anywhere in the Carlton Rhyolite Group occur in the felsitic center of flow BM3 (Figs. 8A and 8B). Excellent exposures of the interior of the flow along the ridge at the top of Bally Mountain reveal that many of the sheeting joints are markedly curved and are disposed in concentric arrays up to several meters across. Where two or more sets of the concentrically arranged joints intersect they form narrow, elongate, spear-like pieces of rhyolite a few centimeters wide. In the upper part of flow BM3, the complex sheeting

joints give way across a well-defined contact to a zone of flow parting with consistent orientations parallel to the top of the flow (Fig. 10).

Ham et al. (1964) interpreted the lower part of flow BM9 to represent a welded ignimbrite, but our field and petrographic observations lead to a different conclusion. The lower ~13 m of the unit has a dark-gray to black groundmass of altered glass. Perlitic texture is visible in thin section and overprints a delicate flow lamination. In the lowest exposed part of the unit, pumiceous rhyolite debris is intermixed on a fine scale with disaggregated vitric tuff. Elongate vesicles in the pumice are outlined by hematite dust and filled by fine-grained secondary quartz; there is no evidence for welding of the pumice or thermal alteration of the intermixed tuff. Streaks, shreds, and tabular clasts of vitric tuff as much as 4 cm long are intermixed with rhyolite in the lower 7 m of the flow. Vesicles decrease in abundance upward and disappear 8.5 m above the base. We interpret these rocks to represent flow pumice that developed in the lower parts of flow BM9 and formed peperite by thorough mixing with underlying unconsolidated vitric ash. No remnants of intact tuff are preserved, and the ash appears to have been completely disrupted during peperite formation. Tuff also occurs as the host to small areas of peperite at the base of flow BM6 (Fig. 10), but no intact intervals of tuff are preserved beneath that flow either.

### ***Bedded Volcanoclastic Rocks between Flows BM2 and BM3***

Relatively thick sequences of bedded volcanoclastic rock occur in two parts of the Bally Mountain section. On the southwest side of Bally Mountain (Figs. 10 and 11), flow BM3 rests on bedded rhyolitic volcanoclastic rocks first recognized by Ham et al. (1964) and described in more detail by Cross (2002). These rocks become covered to the northwest and then reappear on the smaller hill directly northwest of Bally Mountain, where they are 100 m thick. Measured sections from two different locations in these rocks are shown in Figures 12 and 13. Much of the interval is covered, but sufficient exposures allow documentation of the main rock types and sedimentary features.

Planar-bedded volcanoclastic sandstone, vitric tuff, and brown to tan tuffaceous mudstone and siltstone make up much of the sequence. Beds tend to be tabular on the scale of individual outcrops (Fig. 14A), although erosional scour is present at the base of some beds. The coarser beds are typically separated by thin interbeds of brown to tan tuffaceous siltstone containing rhyolite lithic particles and variable amounts of terrigenous mud mixed with some

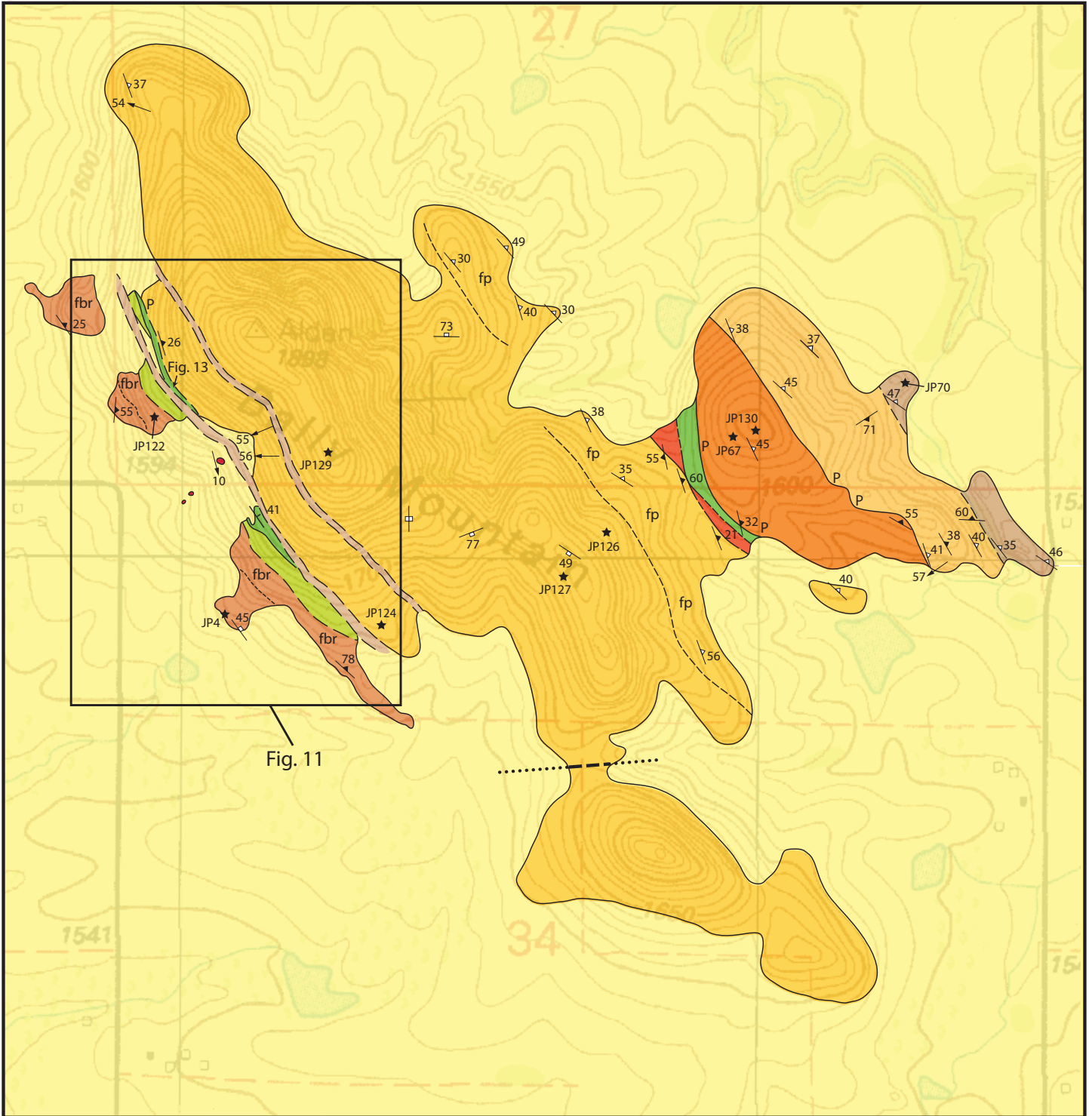
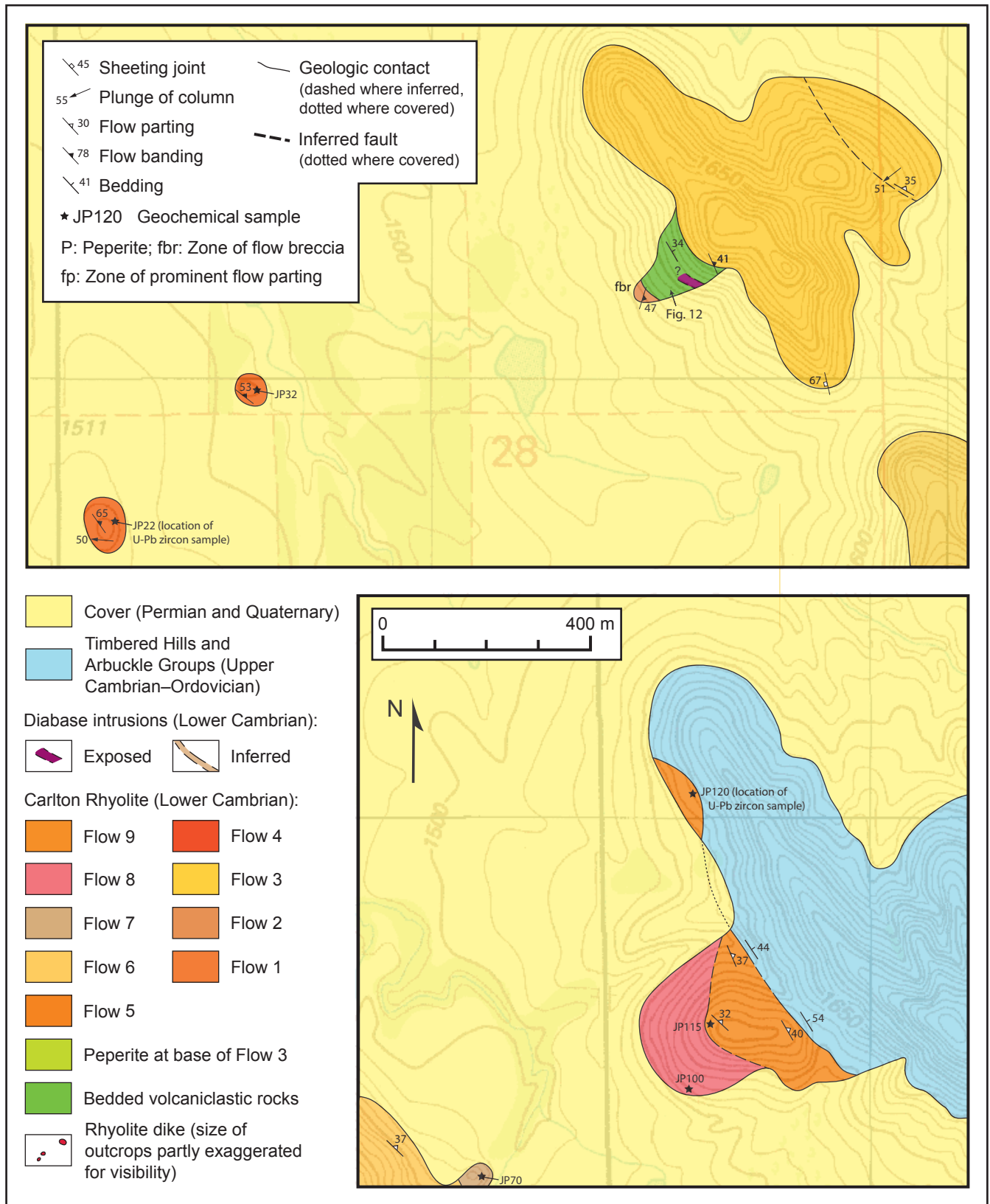
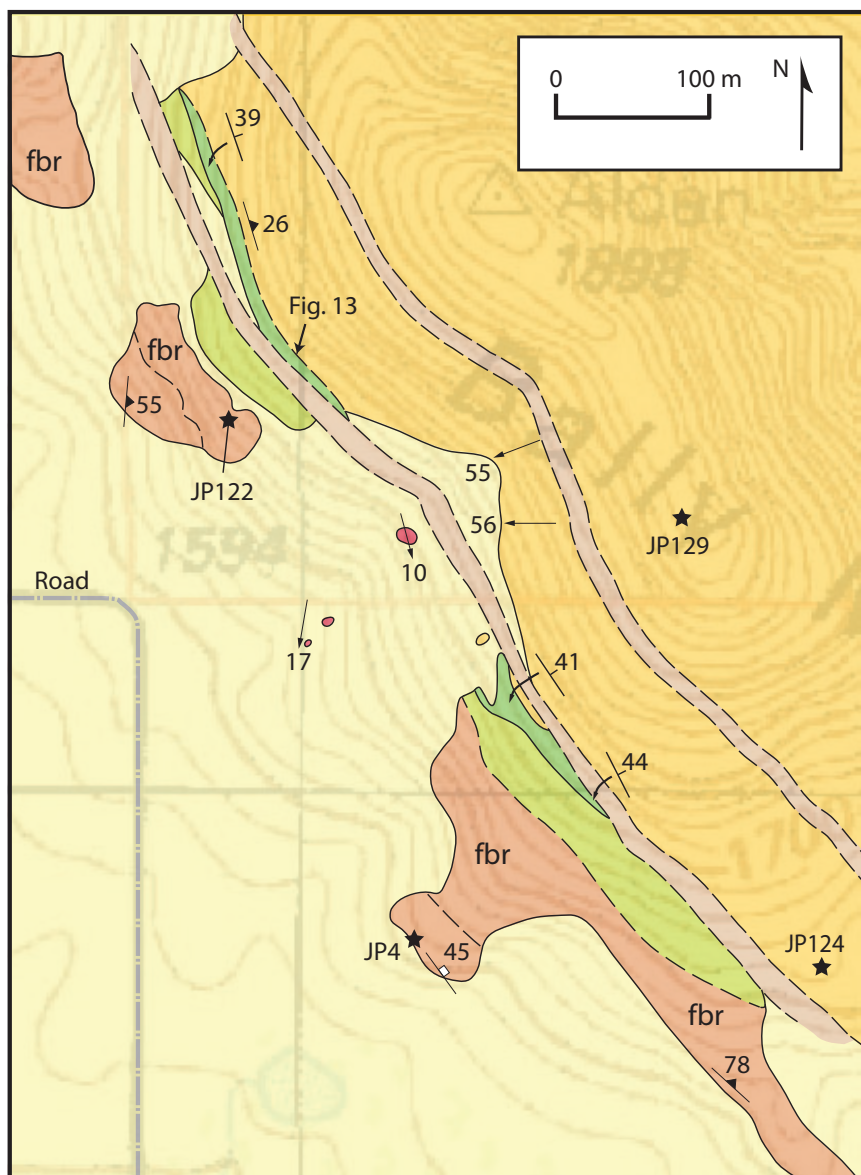


Figure 10. Geologic map of the Carlton Rhyolite in the Bally Mountain area based on unpublished mapping by Hanson and Pollard. See Figure 2 for relative locations of the different parts of this map. Locations of Figures 11, 12, and 13 are indicated.

Physical volcanology of the Carlton Rhyolite, Wichita Mountains





**Figure 11. Detailed map of features exposed on the lower southwest slopes of Bally Mountain. See Figure 10 for location and map legend. Based on unpublished mapping by Hanson, Frazier, and Pollard.**

bubble-wall shards. These beds typically show normal grading and/or delicate planar lamination (Fig. 14B). Many of the fine-grained beds have sharp bases and grade up into tuffaceous mudstone with delicate planar lamination. Thin interbeds of vitric tuff contain abundant tricusate shards and are interpreted as primary ash-fall deposits. Other layers show cross-lamination in places (Fig. 14B), recording slight reworking of ash after deposition.

The sandstones range from fine-grained to very coarse grained, and some are pebbly in their lower parts. They contain rhyolite lithic grains, feldspar and quartz crystals

and, in some cases, small amounts of altered bubble-wall shards, indicating a component of reworked volcanic ash. Normal grading is common and passes up into thin, planar-laminated zones in the upper parts of some beds; inverse grading near the base of beds is less common. Other sandstone beds are massive or have diffuse internal bedding planes defined by changes in grain size. The coarsest units are clast- to matrix-supported debris-flow deposits that are massively bedded or show coarse-tail normal grading. The most notable example is 28 m thick (Fig. 12) and contains angular to subrounded clasts as much as 1.2 m in length. Rhyolite clasts within the debris-flow deposits show a range of phenocryst contents and groundmass textures and are set within a matrix of terrigenous mud intermixed with the same types of sand-sized particles as present in the sandstones. One of the deposits also contains a basalt clast 4.5 mm across that has randomly arranged plagioclase microlites in a tachylitic groundmass.

The planar bedding within the sequence and the lack of tractional current structures in all but the finer grained beds argues against a fluvial origin. The sedimentary features are best explained by deposition in a lake with intermittent influx of subaqueous debris flows and high-concentration turbidity currents. The lake apparently was deeper to the northwest where the thickest part of the volcanoclastic interval is preserved. Thin interbeds of graded to planar-laminated siltstone and tuffaceous mudstone record suspension sedimentation of finer grained particles in quiet water between introduction of the coarser sediment-gravity

flows; in some cases, fine-grained volcanic ash from distant eruptions also settled through the water column onto the lake floor. Quartz phenocrysts in the rhyolite clasts within these deposits are in many cases more abundant than in the two stratigraphically underlying rhyolite flows (BM1 and BM2), indicating that at least some of the rhyolite debris came from more distant sources. The presence of the basalt clast in one debris-flow deposit is significant because it suggests that at least a small amount of basalt lava was intercalated with the rhyolites in the source region for the sediment-gravity flows that entered the lake.

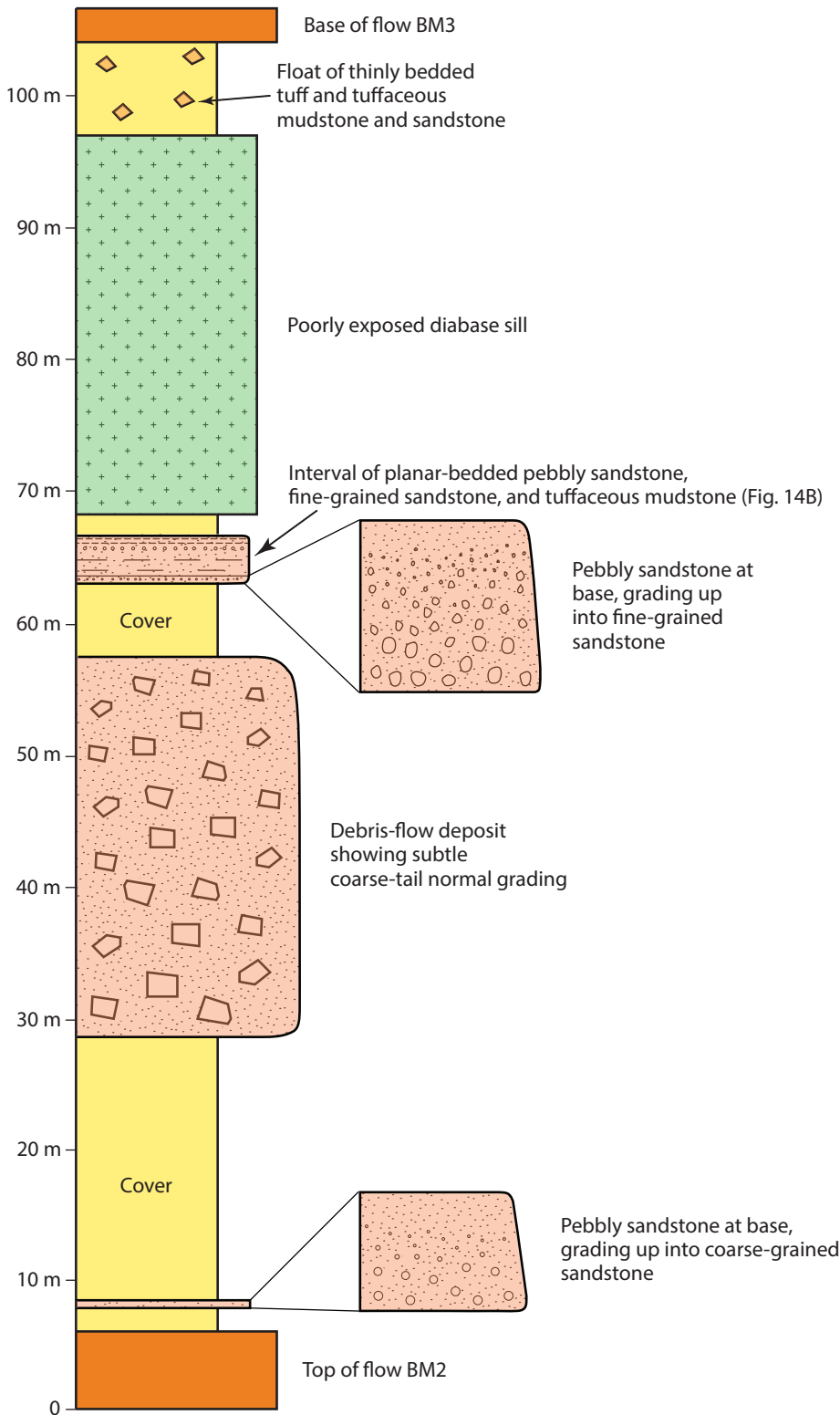


**Figure 12.** Measured section of thickest part of bedded volcanoclastic sequence beneath flow BM3 on Bally Mountain, from Cross (2002). See Figure 10 for location.

***Bedded Volcanoclastic Rocks between Flows BM4 and BM5***

A second poorly exposed volcanoclastic sequence overlies flow BM4 along an erosional contact. Most of the sequence consists of a massively bedded unit containing rhyolite lithic and pumice clasts  $\leq 8$  mm long supported by a matrix rich in broken bubble-wall shards and loose crystals of feldspar and quartz. The shards and pumice are replaced by very fine grained quartz, alkali feldspar and green clay. Welding or other evidence of heat retention is absent. This unit may represent a pyroclastic-flow deposit that was too small to retain sufficient heat for welding, or it may have formed when loose pyroclastic material was mixed with water and transported to the depositional site as a cold debris-flow deposit. The deposit is as much as 30 m thick and occupies a channel cut into flow BM4, with the deepest part of the channel extending down to the top of flow BM3 (Fig. 10). Presumably the channel was cut by stream activity and served as a conduit for the gravity-driven particulate flow. The deposit is overlain by 5 m of planar-laminated, very fine grained crystal-vitric tuff. Peperite is developed along the contact between the tuff and the base of flow BM5, and clasts and irregular small intrusive tongues  $\leq 8$  mm across derived from that flow are locally present throughout the entire thickness of the tuff.

***Extensive Peperite at the Base of Flow BM3***

An unusually extensive zone of peperite occurs on the southwest side of Bally Mountain beneath flow BM3 (Fig. 11). In places, the base of the flow rests directly on the underlying lacustrine strata without noticeable disturbance of the bedded rocks or with only local development of small areas of peperite. More extensive zones of peperite as much as 20 m thick occur beneath the undisturbed lacustrine strata. In the southeast part of the area shown in Figure 11, the bedded strata are absent and their place is taken by the peperite,

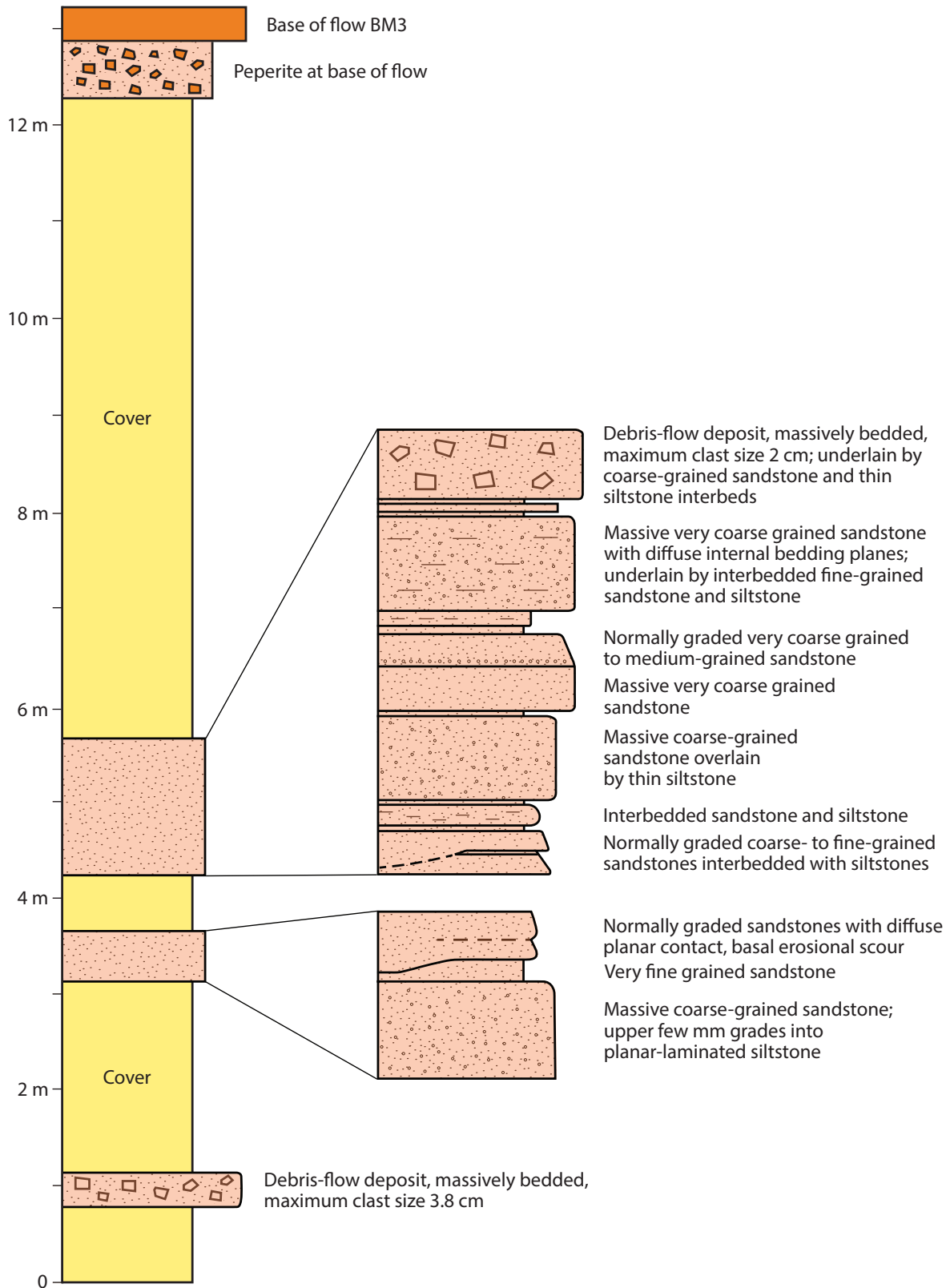


**Figure 13. Measured section of thinner part of bedded volcanoclastic sequence beneath flow BM3, from Cross (2002). See Figures 10 and 11 for location.**



which is separated from the base of flow BM3 by a grass-covered bench believed to represent a diabase intrusion, as discussed earlier. The rhyolite in these larger peperite zones is petrographically identical to flow BM3, which has larger and more abundant quartz phenocrysts than flow BM2. The peperite is in sharp contact with flow breccia in the upper part of flow BM2, and the contact can be readily mapped based on the presence of sediment between clasts in the peperite and the differences in phenocryst contents between the two flows.

The peperite consists of rhyolite fragments dispersed to various degrees within thoroughly disrupted, brown-colored tuffaceous mudstone. Some rhyolite fragments have fluidal outlines (Fig. 15A) that record the tearing apart of viscous lava during peperite formation. More commonly, the rhyolite fragments are sharply angular (Figs. 15B and 15C), indicating brittle failure of rapidly quenched lava. A similar range in clast types occurs in other examples of peperite described in the literature (e.g., Busby-Spera and White, 1987; Hanson and Hargrove, 1999; Skilling et al., 2002). Smaller angular rhyolite pieces can be matched together like pieces of a jigsaw puzzle (Figs. 15B and 15C), recording non-explosive, in situ quench fragmentation. Larger rhyolite fragments are penetrated along thermal contraction fractures by thin tendrils of sediment and fine-grained rhyolite shards (Fig. 15B). Similar features in other peperites are attributed to fluidization of the host sediment by rapid conversion of pore water to steam (Kokelaar, 1982). A model to explain the formation of the peperite is shown in Figure 16. As flow BM3 moved across wet, unlithified, mechanically weak lacustrine sediments, one or more tongues from the base of the flow penetrated down into the sediments and propagated laterally, forming a peperite sill beneath the flow.



**Figure 14. (A) View looking southeast at part of bedded volcanoclastic sequence southeast of location of Figure 13. Sandstone beds form prominent shelves. Outcrops of flow BM3 are visible on the slope above. (B) Loose piece of tuffaceous sandstone showing planar and low-angle cross lamination. Location shown in Figure 12.**

In their measured section Ham et al. (1964) depicted an interval of what they termed “flow breccia or agglomerate” be-

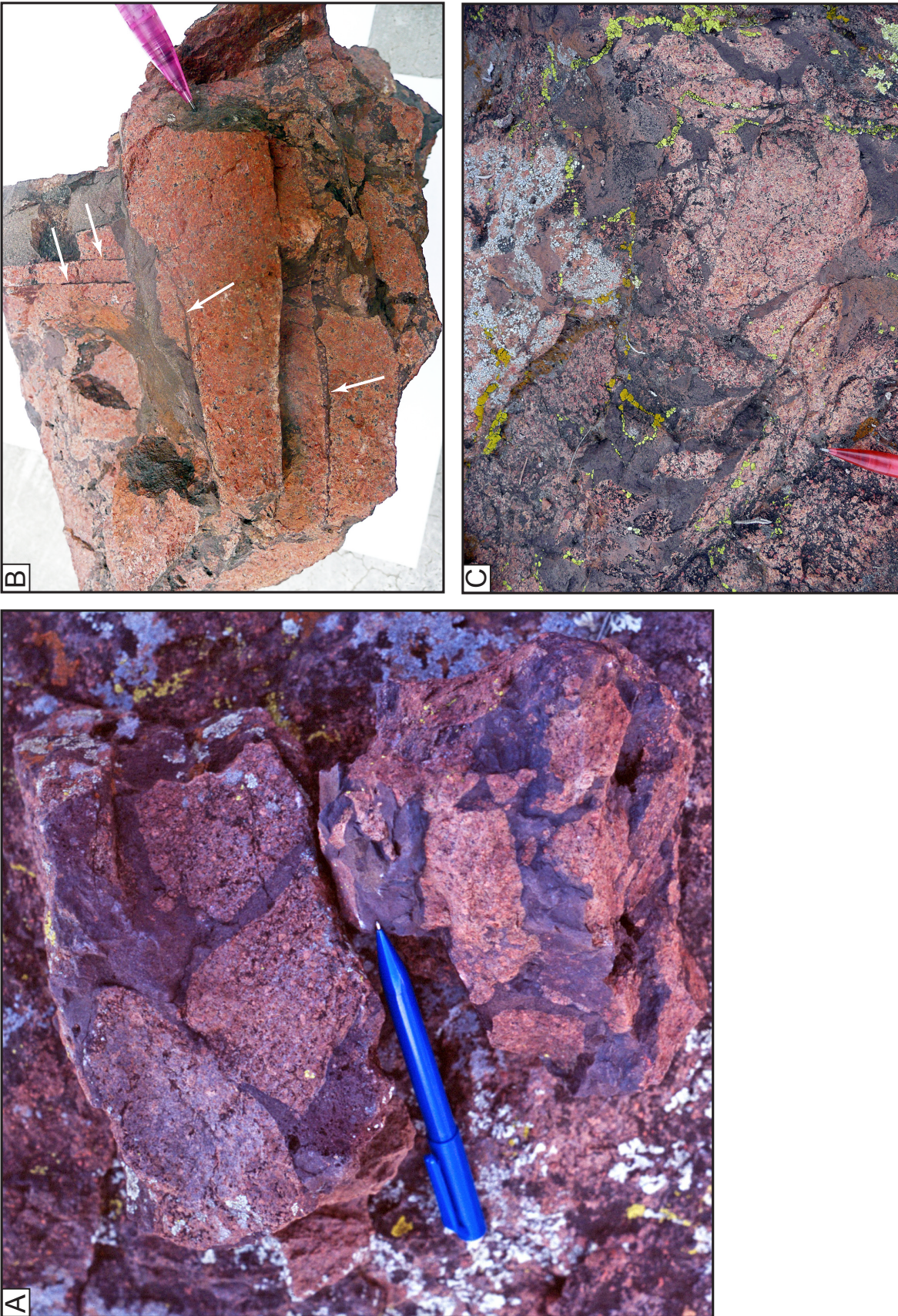


Figure 15. (A) Peperite at base of flow BM3 showing rhyolite clasts with fluidal to angular shapes intermixed with brown tuffaceous mudstone. (B) Sample of peperite with angular rhyolite clasts penetrated by thin fractures (arrows) filled with host sediment (brown) and fine-grained particles of shattered rhyolite. (C) Rhyolite clasts within peperite showing in situ fragmentation.

neath the bedded volcanoclastic sequence on the southwest side of Bally Mountain. This interval corresponds to what we have mapped as flow breccia at the top of flow BM2 as well as the peperite sill beneath the bedded volcanoclastic rocks. The photograph of a sample from this interval given in Ham et al. (1964, fig. 5) is very similar to parts of the peperite and undoubtedly comes from that unit. At the time of their work, there were few reports of peperite in the English literature and only more recently has it been recognized to occur commonly in a variety of volcanic settings (e.g., Skilling et al., 2002).

### **Rhyolite Feeder Dike**

Our detailed mapping in the area of Figure 11 has also revealed the presence of a discontinuously exposed rhyolite dike beneath flow BM3. The dike forms three relatively small outcrops in an otherwise covered area along a drainage. Columnar jointing is developed perpendicular to the dike margins and shows a markedly different orientation from columnar jointing at the base of flow BM3. The largest outcrop, which is 5.7 m across, apparently exposes the entire width of the dike because chilled margins are preserved along both sides of this outcrop, although the adjacent country rock is covered. The chilled margins show development of small spherulites  $\leq 0.5$  mm in width that disappear toward the dike interior, which consists of homogeneous felsite. Phenocryst contents in the dike are virtually identical to those in BM3. We cannot trace the dike directly into the base of flow BM3 because of lack of outcrop, but a careful search of exposures on the southwest side of Bally Mountain indicates that the dike does not continue at higher levels. We therefore conclude that the dike represents a feeder for flow BM3, the first of its kind to have been found in the Carlton Rhyolite Group. Whether a dike only 5.7 m across could have been the sole feeder for flow BM3, which is 370 m thick, is unclear. A flow this large was possibly fed by more than one dike.

### **Northwest Bally Mountain Area**

Parts of eight rhyolite flows are exposed in several hills northwest of Bally Mountain (Fig. 17; Frazier et al., 2012). Although flow bases or tops are only partly exposed, it is clear that most of these flows are significantly thinner than those on Bally Mountain, and none of the flows can be directly correlated between the two areas. We infer that the two areas are separated by a covered fault (Fig. 2). The amount and sense of displacement on this fault are unknown. Grass-covered benches occur between flows NBM4

and NBM5 and between flows NBM6 and NBM7. They are similar in appearance to the benches on the southwest side of Bally Mountain and, like those examples, are believed to represent intrusive diabase sheets not exposed at the surface.

Flow banding and flow folding are well developed in most of the flows and pass into flow breccia at flow bases and tops (Fig. 17). Flows NBM2 and NBM6 lack internal felsitic zones, possibly because they were too thin to undergo the slower cooling required to form felsitic rhyolite. Felsitic zones in the other flows are typically substantially thinner than in the Bally Mountain flows.

Thin zones of peperite occur at the base of flows NBM2 and NBM5 and contain rhyolite clasts intermixed with vitric tuff preserving bubble-wall shards (fig. 12 in Hanson and Eschberger, this guidebook). A sequence of bedded rhyolitic volcanoclastic rocks 10 m thick separates flows NBM3 and NBM4. It is relatively poorly exposed but appears to consist predominantly of planar-bedded, clast- to matrix-supported debris-flow deposits intercalated with intervals as much as 4.5 m thick comprising fine- to coarse-grained volcanoclastic sandstone and siltstone, brown mudstone, and light-gray vitric tuff preserving delicate planar lamination. The debris-flow deposits contain several types of angular rhyolite clasts  $\leq 15$  cm across. Where individual deposits can be discerned they are  $\leq 40$  cm thick and are separated by thin mudstone layers. The characteristics of this bedded volcanoclastic sequence suggest deposition in a lacustrine setting similar to that recorded by the thicker sequence beneath flow BM3 at Bally Mountain. Peperite is absent in the sequence in the northwest Bally Mountain area, but tuffaceous rocks within it locally show soft-sediment folding, probably induced by emplacement of the overlying rhyolite lava on wet, unconsolidated sediment.

Flow NBM4 contains a local area of well-developed columnar jointing in which the columns plunge at a relatively low angle to the northeast (Fig. 17), in marked contrast to the columnar jointing in most of the rhyolite flows in the Slick Hills which is developed perpendicular to flow bases and tops. This anomalous area may represent a flow lobe developed near the lateral margin of the flow. Similar features occur near the lateral terminations of Miocene A-type rhyolite lava flows in the Snake River Plain (Bonnichsen and Kauffman, 1987), although the lobes developed in the Miocene lavas are considerably larger than the example described here. The presence of this possible flow lobe and the fact that the northwest Bally Mountain flows are thinner than many of the flows elsewhere in the Slick Hills suggest that the rhyolites in the northwest Bally Mountain area may represent a more distal lithofacies as-

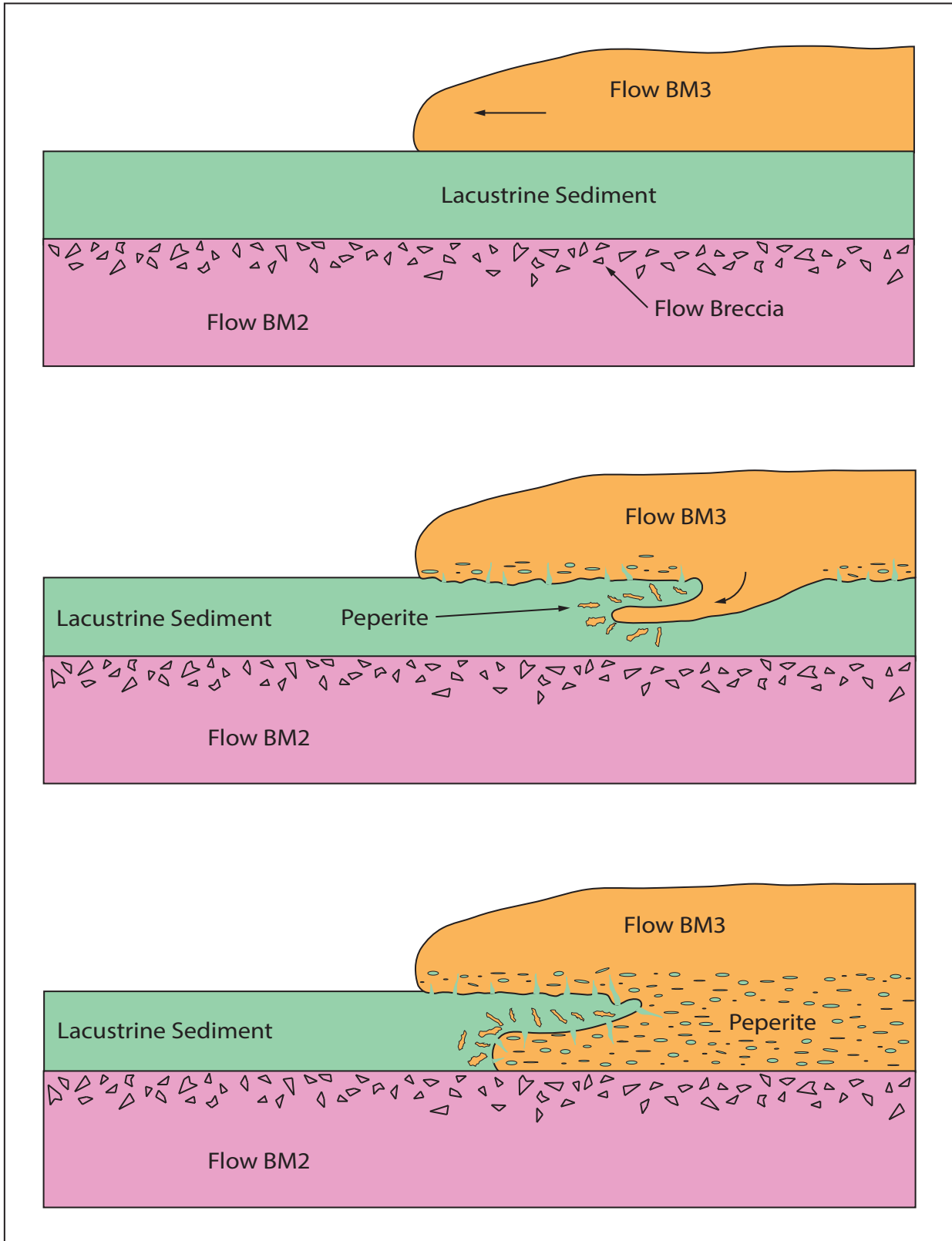


Figure 16. Diagram showing development of peperitic sill extending from base of flow BM3 into underlying lacustrine sequence. Not to scale.

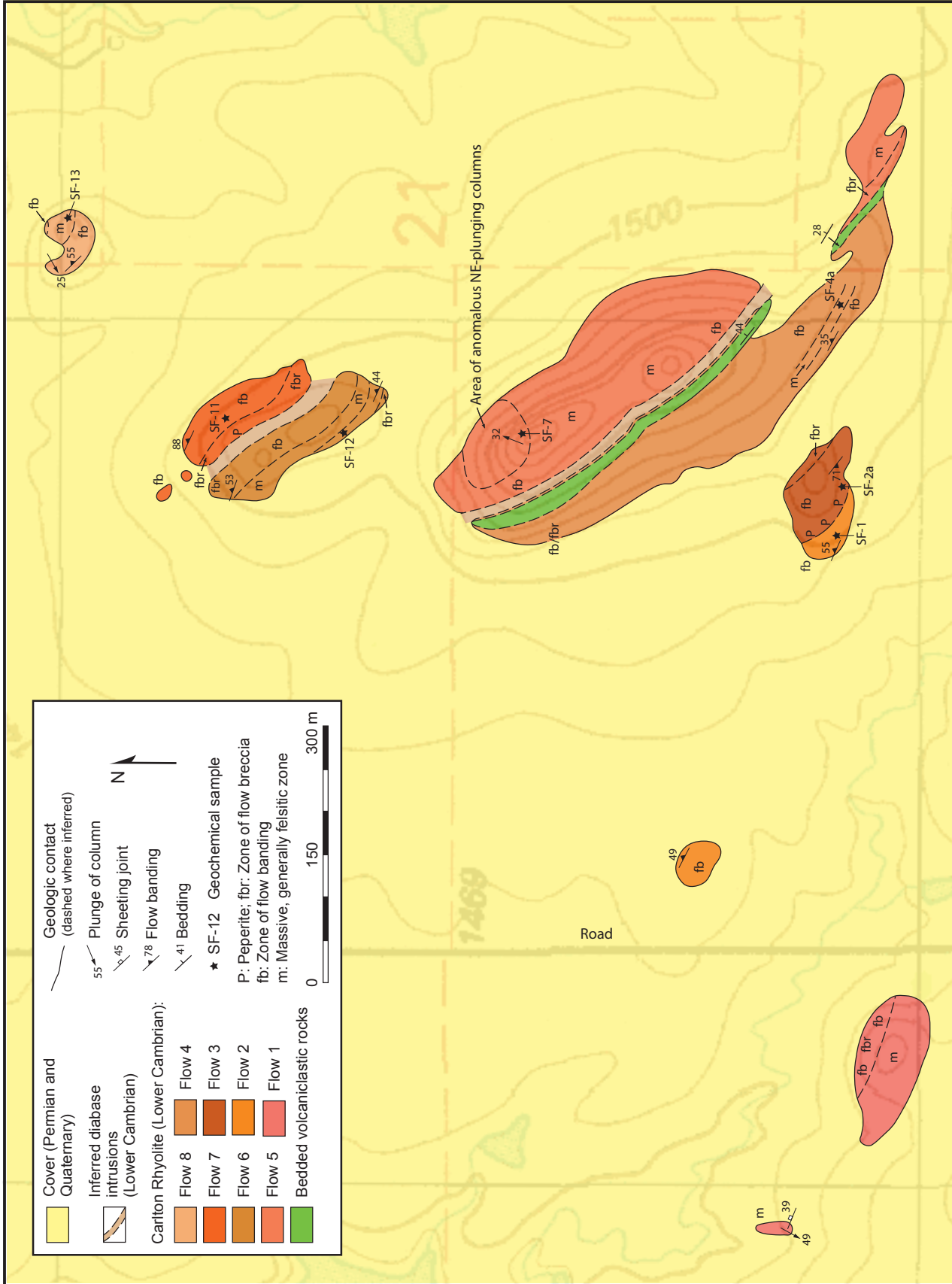


Figure 17. Geologic map of the Carlton Rhyolite in the northwest Bally Mountain area based on unpublished mapping by Hanson, Frazier, and McCleery. See Figure 2 for location.

semblage that has been juxtaposed against the Bally Mountain area to the south by faulting.

### Zodletone Mountain Area

The overall geological setting of Zodletone Mountain is discussed in Donovan et al. (1988b). Mapping by Burkholder (2005) shows that four rhyolite flows are exposed on the mountain, two of which are cut by northwest-striking diabase dikes (Fig. 18). We also group another rhyolite flow that crops out on a small knob to the southwest (Fig. 2) as part of the Zodletone Mountain succession and term it flow ZM1. Only the lower part of flow ZM1 is exposed and consists of pervasively flow-laminated rhyolite with finely developed spherulitic texture visible in thin section in the groundmass. The stratigraphically lowest outcrops show perlitic texture, suggesting they are near the original glassy base of the flow. Flows ZM2 and ZM3 crop out in the western part of Zodletone Mountain, but because of poor exposure it has not been possible to map out the boundary between these two flows or their internal zonation in detail; they are therefore shown as a single color in Figure 18. Only the upper 40 m of flow ZM2 is exposed along the southwest base of the mountain and shows flow banding that becomes less well defined lower in the flow.

Flows ZM3 and ZM5 exhibit the standard vertical zonation shown in Figure 3, and their felsitic interiors hold up the high points in the areas where the flows crop out. Columnar jointing in the felsitic zones in some cases is perpendicular to flow bases and tops but in other cases shows variations in plunge direction (Fig. 18). Flow ZM4 departs from the general flow model in that it lacks a felsitic interior and some originally glassy areas with perlitic texture occur in the central part of the flow. Most of the flow shows well-developed flow banding and flow lamination with thicker bands defined partly by coalescing spherulites and thinner laminae defined by color variations. Flow folds with wavelengths of meters to tens of meters are common. Flow breccia occurs locally at the top of the flow and is also locally present within the flow interior. Peperite is discontinuously developed along the base of the flow, which is defined by a distinct topographic saddle. The peperite consists of rhyolite intermixed with thin lenses or tongues of very fine grained vitric tuff that locally preserves planar lamination. A thick zone of flow breccia occurs above the peperite and passes up into the flow-banded flow interior. Small, irregular areas of peperite occur within the flow breccia well above the base of the flow, where disrupted tuff similar to that below surrounds clasts of rhyolite.

The base of the stratigraphically highest flow on Zodletone Mountain (flow ZM5) is only well exposed in one area where it is separated from flow ZM4 by an interbed of fine-grained crystal-vitric rhyolite tuff ~1 m thick that can be traced for ~10 m along strike before becoming covered. Rhyolite just above the tuff shows flow lamination parallel to the contact with no development of peperite. Flow banding in the lower part of the flow passes upward into the thick felsitic interior of the flow. The top of flow ZM5 is covered, but small outcrops and locally derived float near the northeast mapped limit of the flow consist of gray-green, originally glassy rhyolite with perlitic texture, indicating that the stratigraphically highest exposures of the flow are near the transition into the upper chilled margin.

### GEOCHEMISTRY

Complete chemical analyses are available for most of the rhyolite flows we have mapped in the Slick Hills (Table 2). Volatile-free silica values for the flows range between 70.13 and 75.67 wt % (volatile-free). On the Harker diagrams in Figure 19, TiO<sub>2</sub>, Al<sub>2</sub>O<sub>3</sub>, FeO, and P<sub>2</sub>O<sub>5</sub> contents define reasonably coherent trends that show general decreases with increase in SiO<sub>2</sub>. The hypabyssal rhyolite intrusion in the Blue Creek Canyon area plots well apart from the flows and represents a separate, less-evolved batch of magma. MgO values for the samples as a whole are uniformly low but are somewhat scattered, suggesting that Mg was more susceptible to secondary alteration than some of the other major elements. CaO values generally show a coherent trend, with the exception of several samples that plot above the general array of data. Two of these samples (JP4 and JP122, both from flow BM2) contain secondary calcite in thin section, which occurs filling small amygdules and in irregular patches replacing parts of the groundmass. The other samples with higher than normal CaO contents, however, lack obvious evidence for addition of calcite.

The alkalis show clear evidence of mobility during alteration, with four samples in the Hughes (1972) diagram in Figure 20A falling outside the normal igneous spectrum. Sample JP120 from flow BM9 has such a high ratio of K<sub>2</sub>O to Na<sub>2</sub>O that it plots off the scale of the diagram. In that particular sample, the feldspar phenocrysts are nearly completely replaced by sericite, which also forms disseminated flakes in the groundmass. The sample was collected a short distance below the unconformity with Upper Cambrian and Ordovician sedimentary strata, and the strong alteration shown by the sample may be the result of preferential fluid flow along the unconformity. Another sample (sample

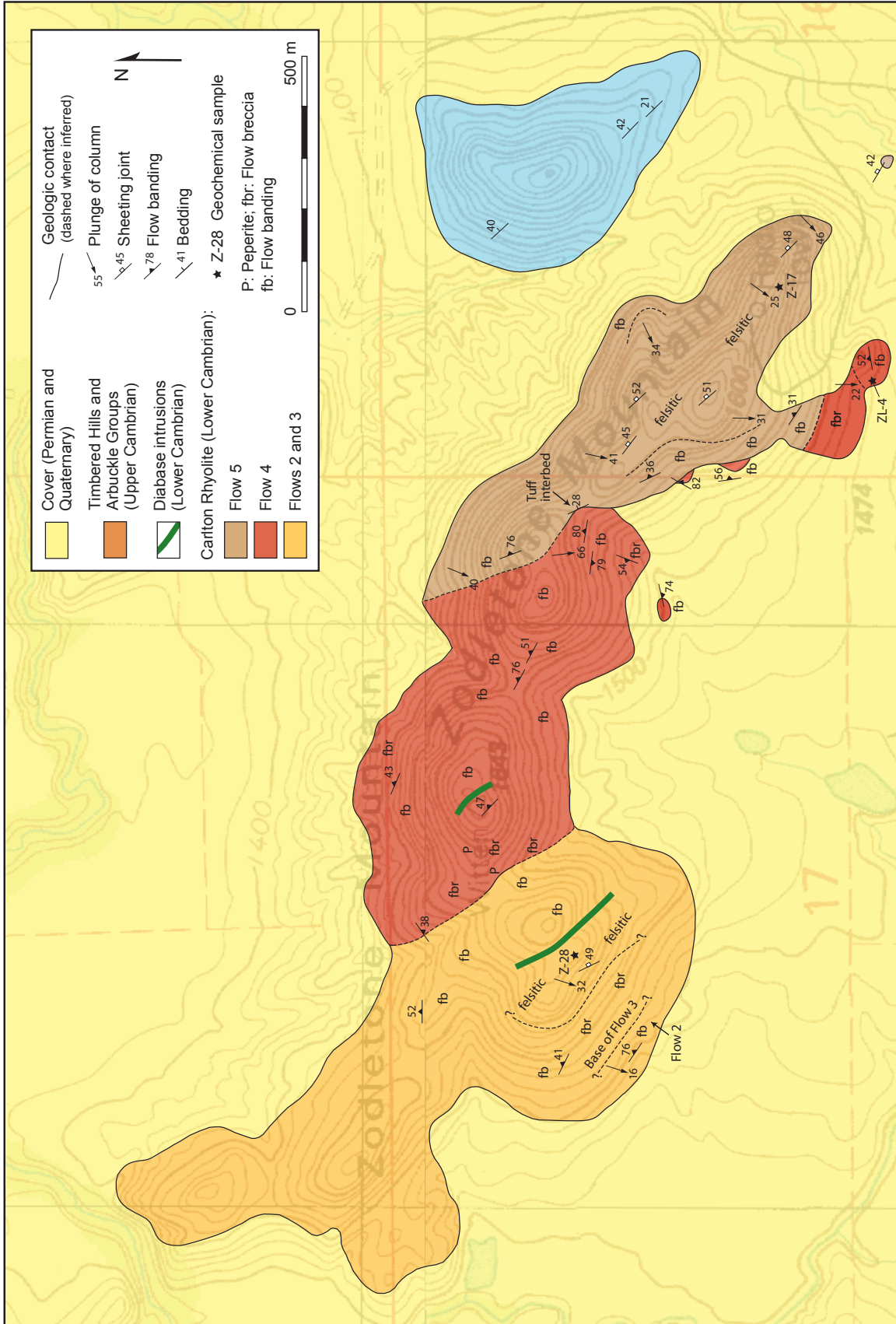


Figure 18. Geologic map of the Carlton Rhyolite on Zodletone Mountain modified from Burkholder (2005). See Figure 2 for location.

TABLE 2: GEOCHEMICAL DATA FOR CARLTON RHYOLITE IN THE SLICK HILLS

Normalized major elements (wt %)*												
Sample	JP 22	JP 32	JP 4	JP 122	JP 124	JP 126	JP 127	JP 129	JP 67	JP 130	JP 70	JP 100
Flow	BM1	BM1	BM2	BM2	BM3	BM3	BM3	BM3	BM5	BM5	BM7	BM8
SiO <sub>2</sub>	74.78	72.39	72.44	74.28	73.01	73.24	73.00	72.95	72.85	73.68	71.67	72.69
TiO <sub>2</sub>	0.49	0.53	0.55	0.40	0.47	0.46	0.45	0.46	0.52	0.43	0.59	0.48
Al <sub>2</sub> O <sub>3</sub>	12.54	13.23	12.84	12.88	12.93	12.94	12.87	12.94	12.82	12.58	13.15	13.04
FeO	3.53	4.51	4.39	3.17	4.05	4.40	4.02	3.89	4.51	4.31	4.54	4.32
MnO	0.03	0.07	0.05	0.08	0.06	0.05	0.08	0.09	0.04	0.03	0.07	0.05
MgO	0.28	0.53	0.35	0.43	0.71	0.36	0.52	0.49	0.49	0.28	0.50	0.83
CaO	0.42	0.39	1.26	0.83	0.91	0.29	0.60	0.67	0.31	0.32	0.75	0.35
Na <sub>2</sub> O	3.12	3.97	3.54	3.21	3.26	4.04	3.89	3.82	3.93	4.01	4.55	4.16
K <sub>2</sub> O	4.70	4.25	4.46	4.64	4.52	4.13	4.47	4.60	4.42	4.27	4.06	4.00
P <sub>2</sub> O <sub>5</sub>	0.10	0.12	0.11	0.08	0.10	0.09	0.09	0.09	0.10	0.08	0.13	0.09
LOI**												
Total***	99.66	99.89	99.35	99.25	99.14	99.46	99.37	99.16	99.06	99.49	99.31	99.10
Trace elements (ppm)												
Ba	804.00	781.00	665.00	1179.00	869.00	781.00	676.00	648.00	860.00	978.00	781.00	538.00
Rb	139.00	125.60	104.20	145.40	128.30	111.70	115.70	119.90	130.70	137.00	114.40	136.80
Nb	79.95	82.42	81.47	72.53	72.94	72.36	69.11	68.78	70.69	70.59	71.94	86.92
Ta	5.38	5.83	5.94	5.09	4.84	4.87	5.29	4.79	5.32	5.31	4.96	6.48
Sr	20.00	24.00	21.00	48.00	60.00	60.00	48.00	37.00	54.00	80.00	55.00	13.00
Zr	644.00	680.00	675.00	657.00	664.00	652.00	582.00	523.00	539.00	554.00	564.00	655.00
Y	81.28	93.86	105.10	96.04	93.65	91.12	84.96	80.86	92.83	97.81	102.13	84.78
Sc	7.80	8.20	8.70	10.90	11.30	11.20	9.40	8.20	8.90	9.00	9.40	7.90
Cr	1.00	3.00	0.00	0.00	0.00	3.00	1.00	8.00	0.00	0.00	1.00	1.00
Ni	9.00	14.00	11.00	11.00	12.00	19.00	16.00	13.00	11.00	9.00	13.00	11.00
V	21.00	7.00	22.00	18.00	9.00	13.00	13.00	9.00	19.00	12.00	14.00	8.00
Cu	6.00	9.00	6.00	0.00	4.00	2.00	1.00	2.00	2.00	5.00	0.00	1.00
Zn	91.00	126.00	111.00	104.00	92.00	85.00	133.00	119.00	111.00	87.00	98.00	108.00
La	76.60	77.76	110.63	71.38	85.84	75.28	80.12	58.49	76.49	83.19	96.07	78.18
Ce	190.50	178.38	178.63	153.53	171.86	161.65	157.06	119.00	159.71	171.97	160.82	164.34
Pr	20.87	19.36	26.91	20.78	22.73	20.73	20.81	17.04	20.55	21.82	23.90	21.29
Nd	79.96	75.16	105.28	84.66	89.47	82.13	82.26	67.84	80.62	85.47	93.42	81.56
Sm	18.33	16.19	23.04	19.60	19.80	18.29	17.75	15.69	18.02	18.60	20.38	17.55
Eu	2.84	2.50	3.70	3.77	3.74	3.40	3.10	2.44	2.87	3.02	3.26	2.67
Gd	16.03	15.45	21.83	18.43	18.43	17.02	16.51	14.68	17.30	17.67	19.54	15.16
Tb	2.96	2.78	3.61	3.14	3.05	2.93	2.83	2.59	2.98	3.01	3.34	2.65
Dy	17.73	17.62	20.86	18.76	18.29	17.82	17.07	15.78	18.19	18.20	20.20	16.63
Ho	3.43	3.59	4.03	3.69	3.59	3.55	3.37	3.20	3.65	3.71	4.04	3.43
Er	9.25	10.07	10.74	9.96	9.77	9.83	9.21	8.85	9.93	10.01	10.68	9.64
Tm	1.37	1.47	1.57	1.42	1.41	1.43	1.35	1.31	1.44	1.45	1.52	1.48
Yb	8.60	9.27	9.68	8.79	8.77	8.92	8.44	8.24	8.96	9.04	9.38	9.27
Lu	1.32	1.42	1.47	1.33	1.32	1.35	1.27	1.26	1.32	1.36	1.42	1.41
Hf	17.01	17.79	17.83	16.65	17.10	16.68	15.56	14.38	14.81	14.99	15.52	17.56
Th	14.46	14.78	14.92	12.73	13.01	12.97	13.17	13.66	14.13	13.81	14.41	14.88
Pb	3.30	8.53	3.70	4.33	7.23	10.80	5.98	5.64	9.07	9.37	5.09	4.96
U	3.88	3.11	3.62	3.02	3.05	3.46	3.55	3.31	3.73	3.62	3.44	3.34
Cs	0.54	0.58	0.37	1.33	1.39	0.61	2.52	1.52	1.44	1.85	0.91	2.37
Ga	22.00	24.00	24.00	24.00	26.00	26.00	22.00	25.00	25.00	23.00	25.00	25.00

\*Major elements are normalized to 100% on a volatile-free basis

\*\*Loss on ignition

\*\*\*Total before normalization

*Physical volcanology of the Carlton Rhyolite, Wichita Mountains*

TABLE 2: GEOCHEMICAL DATA FOR CARLTON RHYOLITE IN THE SLICK HILLS, CONTINUED

Normalized major elements (wt %)*												
Sample	JP 115	JP 120	CP 356A	CP 239A	CP 143	CP 46	CP 197B	CP 350A	CP 351A	CP 352A	CP 196B	CP 355A
Flow	BM9	BM9	BC2	BC3	BC4	BC5	BC5	BC5	BC5	BC5	BC6	Intrusion
SiO <sub>2</sub>	73.98	74.12	71.34	71.65	73.18	73.82	74.55	74.24	74.45	75.67	74.17	70.13
TiO <sub>2</sub>	0.31	0.26	0.60	0.61	0.49	0.33	0.30	0.33	0.31	0.30	0.31	0.37
Al <sub>2</sub> O <sub>3</sub>	12.65	12.14	13.16	12.95	13.05	13.63	12.60	13.02	12.71	12.25	12.70	14.31
FeO	4.17	2.92	4.85	4.98	4.18	4.20	3.66	3.32	3.48	2.96	4.26	5.45
MnO	0.02	0.01	0.08	0.08	0.03	0.08	0.05	0.03	0.06	0.04	0.03	0.11
MgO	0.53	0.31	0.54	0.29	0.12	0.29	0.14	0.14	0.08	0.06	0.16	0.39
CaO	0.31	0.40	0.71	0.67	0.29	0.28	0.28	0.32	0.24	0.18	0.30	0.41
Na <sub>2</sub> O	3.68	0.30	3.98	3.61	3.88	6.08	3.85	4.53	4.04	3.51	3.81	4.74
K <sub>2</sub> O	4.30	9.46	4.61	5.03	4.70	1.25	4.52	4.02	4.58	4.98	4.22	4.02
P <sub>2</sub> O <sub>5</sub>	0.05	0.03	0.12	0.13	0.09	0.06	0.05	0.06	0.05	0.05	0.04	0.07
LOI**												
Total***	99.23	99.54	98.07	98.00	98.10	96.94	97.93	98.03	98.37	98.16	97.58	98.24
Trace elements (ppm)												
Ba	990.00	767.00	988.00	992.00	881.00	775.00	731.00	860.00	973.00	1101.00	875.00	758.00
Rb	140.40	108.10	129.20	148.00	134.20	130.50	123.70	137.20	119.70	137.40	107.20	101.20
Nb	68.40	72.76	71.88	66.65	75.06	68.64	81.07	70.97	69.02	70.86	87.05	84.47
Ta	5.10	4.91	4.91	5.01	5.05	4.51	5.54	4.77	5.05	4.93	6.04	5.94
Sr	98.00	46.00	73.00	79.00	38.00	46.00	23.00	50.00	86.00	77.00	20.00	29.00
Zr	590.00	636.00	538.00	528.00	659.00	631.00	681.00	540.00	625.00	520.00	786.00	807.00
Y	90.91	87.67	93.97	79.37	86.14	80.80	93.38	92.35	76.85	78.79	103.34	110.91
Sc	10.30	10.30	9.40	7.60	9.80	10.80	8.30	8.40	9.40	8.00	10.20	10.90
Cr	1.00	0.00	0.00	0.00	0.00	0.00	0.00	0.00	0.00	0.00	0.00	0.00
Ni	16.00	8.00	6.00	8.00	8.00	8.00	6.00	8.00	9.00	8.00	7.00	9.00
V	4.00	0.00	10.00	2.00	0.00	14.00	17.00	6.00	7.00	0.00	0.00	3.00
Cu	5.00	0.00	0.00	0.00	0.00	0.00	0.00	0.00	0.00	0.00	0.00	0.00
Zn	112.00	29.00	86.00	73.00	78.00	104.00	77.00	80.00	74.00	74.00	88.00	166.00
La	90.34	92.69	105.01	86.05	80.61	41.43	74.71	84.87	68.82	74.38	100.40	95.40
Ce	165.92	181.31	190.67	170.46	174.77	124.23	187.30	173.37	163.13	143.98	146.78	197.60
Pr	23.12	24.06	25.87	21.36	20.60	13.01	22.14	22.04	19.19	18.64	26.74	25.34
Nd	91.51	94.44	101.28	82.60	79.37	53.28	86.94	86.32	76.34	72.25	107.58	99.37
Sm	20.15	19.99	21.67	17.20	16.57	12.83	19.02	18.60	16.62	15.07	23.82	21.62
Eu	3.80	3.50	3.47	3.02	2.78	2.36	3.01	2.90	3.07	2.56	4.35	4.03
Gd	19.01	18.17	19.74	15.63	14.96	12.29	17.08	17.48	15.46	14.00	21.55	20.51
Tb	3.14	2.97	3.19	2.56	2.71	2.35	2.98	2.95	2.57	2.39	3.54	3.52
Dy	18.52	17.52	18.58	15.51	16.76	15.60	18.43	17.57	15.46	14.58	20.88	21.71
Ho	3.61	3.49	3.68	3.16	3.49	3.35	3.74	3.53	3.16	3.01	4.14	4.41
Er	9.45	9.47	10.04	8.84	9.67	9.41	10.27	9.46	8.69	8.37	11.08	11.91
Tm	1.37	1.40	1.47	1.31	1.45	1.40	1.52	1.38	1.29	1.24	1.60	1.73
Yb	8.53	8.91	9.21	8.26	9.21	8.78	9.56	8.60	8.17	7.99	10.12	10.84
Lu	1.28	1.36	1.38	1.24	1.40	1.33	1.44	1.30	1.25	1.20	1.51	1.62
Hf	15.36	16.51	14.81	13.97	17.23	16.27	18.04	14.64	16.07	13.92	20.09	20.54
Th	12.78	13.54	14.24	13.18	14.02	12.46	14.81	14.00	13.20	13.33	14.28	14.62
Pb	10.01	4.55	7.08	9.74	4.33	8.54	3.93	7.11	10.40	14.11	4.43	5.08
U	2.86	3.54	3.71	3.13	3.51	3.51	3.24	3.74	2.95	3.44	3.97	3.96
Cs	1.72	0.77	2.56	2.09	6.11	3.93	0.51	1.05	1.78	3.14	0.63	0.80
Ga	28.00	24.00	25.00	24.00	24.00	25.00	26.00	22.00	25.00	24.00	27.00	35.00

\*Major elements are normalized to 100% on a volatile-free basis

\*\*Loss on ignition

\*\*\*Total before normalization

TABLE 2: GEOCHEMICAL DATA FOR CARLTON RHYOLITE IN THE SLICK HILLS, CONTINUED

Normalized major elements (wt %)*											
Sample	SF 9A	Z 28	ZLF 4	Z 17	SF 1	SF 2A	SF 4A	SF 7	SF 12	SF 11	SF 13
Flow	ZM1	ZM2	ZM3	ZM4	NBM2	NBM3	NBM4	NBM5	NBM6	NBM7	NBM8
SiO <sub>2</sub>	72.05	73.93	72.82	72.94	74.49	72.56	73.27	75.00	74.24	74.85	73.40
TiO <sub>2</sub>	0.59	0.45	0.58	0.44	0.37	0.56	0.55	0.44	0.40	0.36	0.59
Al <sub>2</sub> O <sub>3</sub>	12.72	12.69	12.69	12.65	12.64	12.89	12.31	12.05	12.23	12.15	12.23
FeO	4.68	3.47	4.03	4.30	3.36	4.61	4.68	3.55	3.71	3.45	4.92
MnO	0.08	0.06	0.07	0.05	0.03	0.07	0.04	0.06	0.04	0.02	0.07
MgO	0.75	0.41	0.33	0.81	0.17	0.32	0.35	0.28	0.47	0.30	0.38
CaO	1.05	0.35	0.22	0.33	0.46	0.75	0.21	0.77	0.19	0.17	0.29
Na <sub>2</sub> O	3.62	3.86	3.04	3.36	3.53	3.64	2.46	4.45	2.61	3.23	4.16
K <sub>2</sub> O	4.35	4.69	6.09	5.06	4.89	4.49	6.00	3.32	6.04	5.40	3.84
P <sub>2</sub> O <sub>5</sub>	0.12	0.08	0.13	0.08	0.07	0.12	0.12	0.08	0.07	0.07	0.13
LOI**	1.34				0.81	1.25	1.12	1.12	0.85	0.72	1.35
Total***	97.18	98.28	98.03	98.06	98.78	97.28	97.15	97.33	97.37	97.37	97.37
Trace elements (ppm)											
Ba	1029	753.00	714.00	784.00	1127	1068	1374	838	1134	986	692
Rb	125.4	102.00	35.60	136.60	139.2	129.3	144.7	97.1	176.3	152.4	102.2
Nb	73.85	78.84	83.15	69.43	68.92	72.53	68.07	72.46	76.25	74.95	73.75
Ta	4.98	5.28	5.77	4.52	4.79	4.85	4.47	4.85	5.24	5.18	4.86
Sr	86	32.00	62.00	48.00	66	68	49	72	43	51	51
Zr	656	740.00	718.00	631.00	526	632	640	565	532	491	675
Y	93.97	104.68	100.37	80.90	72.51	81.51	75.61	86.35	75.42	76.92	91.54
Sc	9.2	9.50	8.70	10.50	6.3	9.0	8.9	7.6	8.3	7.7	12.0
Cr	4	0.00	1.00	0.00	7	4	5	4	4	6	3
Ni	3	4.00	5.00	4.00	4	3	5	2	4	3	1
V	17	10.00	8.00	9.00	12	14	19	10	11	10	12
Cu	4	17.00	3.00	4.00	3	8	7	3	6	9	3
Zn	129	100.00	99.00	120.00	83	102	121	89	107	80	121
La	84.87	137.01	57.52	41.41	57.33	78.06	73.01	78.64	91.29	96.78	62.71
Ce	187.06	130.60	104.75	121.52	128.69	166.21	177.97	176.32	183.90	202.30	159.78
Pr	22.94	29.86	12.85	12.94	15.07	20.14	20.14	20.92	23.20	22.57	18.50
Nd	90.30	115.09	50.25	52.78	58.36	80.10	79.76	81.38	89.45	83.12	74.99
Sm	19.70	23.97	13.19	12.74	13.01	17.07	17.30	17.55	18.01	16.11	17.08
Eu	3.79	4.27	2.53	2.31	2.25	3.07	3.25	2.77	2.39	2.12	3.03
Gd	18.11	22.18	15.16	12.10	12.25	15.58	15.57	15.92	14.85	13.75	16.31
Tb	3.08	3.67	3.07	2.34	2.24	2.61	2.62	2.78	2.48	2.35	2.83
Dy	18.48	21.01	20.01	15.53	13.98	15.72	15.41	16.96	15.40	14.79	18.04
Ho	3.73	3.97	4.07	3.30	2.88	3.22	3.09	3.42	3.22	3.11	3.72
Er	10.00	10.56	11.22	9.29	8.16	8.85	8.39	9.25	9.06	8.97	10.18
Tm	1.46	1.49	1.65	1.36	1.23	1.32	1.27	1.36	1.37	1.35	1.47
Yb	9.15	9.24	10.20	8.59	7.78	8.31	8.02	8.55	8.65	8.52	9.21
Lu	1.37	1.42	1.54	1.31	1.19	1.27	1.26	1.31	1.28	1.26	1.36
Hf	16.87	19.17	18.79	16.25	14.06	16.30	16.37	14.99	14.92	13.85	17.58
Th	13.87	14.04	14.48	12.25	14.11	13.42	12.90	13.94	14.80	14.59	12.85
Pb	11.43	7.49	23.92	8.56	7.15	6.50	6.11	6.00	6.75	3.37	7.58
U	3.80	3.53	4.03	3.48	3.19	2.93	2.98	3.71	3.91	3.50	3.58
Cs	0.96	1.12	0.89	4.10	2.06	1.80	2.04	0.52	1.45	1.25	5.68
Ga	27	24.00	25.00	28.00	24	24	24	24	23	20	22

\*Major elements are normalized to 100% on a volatile-free basis

\*\*Loss on ignition

\*\*\*Total before normalization

CP46 from flow BC5) has an unusually low K<sub>2</sub>O to Na<sub>2</sub>O ratio (Figs. 19 and 20A), suggesting it experienced significant sodium metasomatism.

We have analyzed two samples each from flows BM1, BM2, BM5, and BM9, four samples from flow BM3 (the thickest flow on Bally Mountain), and five samples from flow BC5 (the thickest flow in the Blue Creek Canyon area). The major oxides for flow BM3 typically show only limited variation in the Harker diagrams (Fig. 19). The same is true for flow BM9, except for the alkalis which, as noted above, have been disturbed in sample JP120 from this flow. The data suggest that these two flows record eruption of magma batches that were homogeneous in major-element compositions. The two samples from flow BM5 show a spread in SiO<sub>2</sub> values, and the sample with higher SiO<sub>2</sub> shows a greater amount of secondary silica veinlets in the groundmass, suggesting that at least some of the variation between the two samples is the result of secondary silicification. In flows BM1, BM2, and BC5, however, there is no clear petrographic evidence for addition of secondary SiO<sub>2</sub> in significant amounts, and the spread in contents of SiO<sub>2</sub> and some of the other major oxides in these flows in Figure 19 probably at least partly reflects primary compositional heterogeneities.

All the samples tend to cluster tightly in standard discrimination diagrams using immobile trace elements (Figs. 20B, 20C, and 20D). There is slightly more spread between samples in Figure 20D. In that diagram the hypabyssal rhyolite intrusion in the Blue Creek Canyon area plots apart from the other data, as it does in the Harker diagrams (Fig. 19). All of the samples show similar patterns in the normalized multi-element diagram in Figure 21A, except for the alkali elements in some cases, consistent with other evidence that these elements have been disturbed during alteration. The REE plots (Fig. 21B) are also generally quite similar.

The other main rhyolite outcrops in the Wichita Mountains besides the Slick Hills occur in the Fort Sill area (Finegan and Hanson, this guidebook). Hanson et al. (2013) showed that samples of rhyolites from the two areas could generally be divided into three distinct groups in certain diagrams using immobile trace elements. These same three groups are apparent in Figure 22, which plots additional samples not shown in Hanson et al. (2013). Two flows occur in the Fort Sill area and are informally termed the Davidson metarhyolite and the Fort Sill rhyolite (Finegan and Hanson, this guidebook). Samples from the Fort Sill rhyolite define Group 1 in Figure 22. The Davidson metarhyolite plots with two flows and the hypabyssal intrusion from the Blue Creek Canyon area, together with flow

BM9 from the Bally Mountain area, to define group 2. The other flows from the Bally Mountain and Blue Creek Canyon areas fall within group 3, along with all the analyzed flows from the northwest Bally Mountain area. As argued by Hanson et al. (2013), these data can be interpreted to indicate that rhyolite flows in the Wichita Mountains were derived from three different sources or magma reservoirs. This interpretation needs to be tested with isotopic data but, if confirmed with further work, would indicate that flows exposed as part of the same local stratigraphic sequence tapped different magma sources.

## REFERENCES CITED

- Bigger, S.E., and Hanson, R.E., 1992, Devitrification textures and related features in the Carlton Rhyolite in the Blue Creek Canyon area, Wichita Mountains, southwestern Oklahoma: *Oklahoma Geology Notes*, v. 52, p. 124-142.
- Bonnichsen, B., and Kauffman, D.F., 1987, Physical features of rhyolite lava flows in the Snake River Plain volcanic province, southwestern Idaho, in Fink, J.H., ed., *The Emplacement of Silicic Domes and Lava Flows*: Geological Society of America Special Paper 212, p. 119-145.
- Branney, M.J., Barry, T.L., and Godchaux, M., 2004, Sheathfolds in reomorphic ignimbrites: *Bulletin of Volcanology*, v. 66, p. 485-491.
- Breitkreuz, C., 2013, Spherulites and lithophysae—200 years of investigation on high-temperature crystallization domains in silica-rich volcanic rocks: *Bulletin of Volcanology*, v. 75, p. 705-720.
- Burkholder, B.K., 2005, *Paleovolcanology of the Carlton Rhyolite, Zolletone Mountain, southern Oklahoma* [B.S. thesis]: Fort Worth, Texas Christian University, 69 p.
- Busby-Spera, C.J., and White, J.D.L., 1987, Variation in peperite textures associated with differing host-sediment properties: *Bulletin of Volcanology*, v. 49, p. 765-775.
- Cross, J., 2002, *Interflow volcanoclastic deposits in the Cambrian Carlton Rhyolite on Bally Mountain in the Slick Hills of southwestern Oklahoma* [B.S. thesis]: Fort Worth, Texas Christian University, 35 p.
- DeGroat, P.J., Donovan, R.N., Hanson, R.E., and Weaver, B.L., 1995, Cambrian diabase and gabbro in the Blue Creek Canyon area, Wichita Mountains, southwestern Oklahoma: *Oklahoma Geology Notes*, v. 55, p. 168-186.
- Donovan, R.N., 1982, Geology of Blue Creek Canyon, Wichita Mountains area, in Gilbert, M.C., and Donovan, R.N., eds., *Geology of the Eastern Wichita Mountains, Southwestern Oklahoma*: Oklahoma Geological Survey Guidebook 21, p. 65-77.
- Donovan, R.N., 1986, Geology of the Slick Hills, in Donovan, R.N., ed., *The Slick Hills of Southwestern Oklahoma—Fragments of an Aulacogen?*: Oklahoma Geological Survey Guidebook 24, p. 1-12.
- Donovan, R.N., 1995, The Slick Hills of Oklahoma and their regional tectonic setting, in Johnson, K.S., ed., *Structural Styles in the Southern Midcontinent, 1992 Symposium*: Oklahoma Geological Survey Circular 97, p. 178-186.
- Donovan, R.N., and Bucheit, A.K., 2000, Marine facies and islands in the Reagan Formation (Upper Cambrian) in the Slick Hills, southwestern Oklahoma, in Johnson, K.S., ed., *Marine Clastics in the Southern Midcontinent, 1997 Symposium*: Oklahoma Geological Survey Circular 103, p. 25-37.

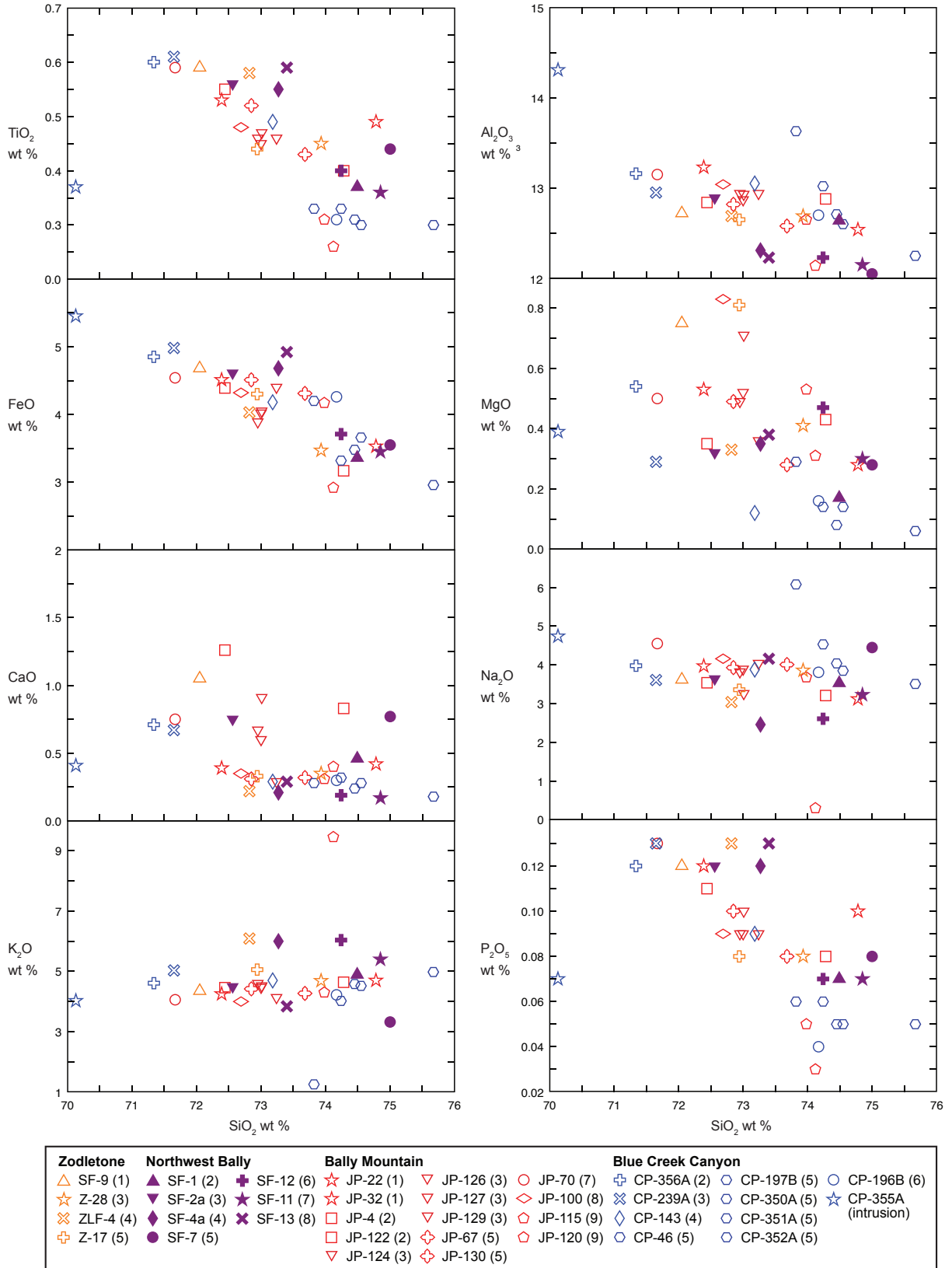


Figure 19. Harker diagrams for major oxides for the Carlton Rhyolite in the Slick Hills. Numbers in parentheses after sample numbers in legend indicate which flows the samples come from.

- Donovan, R.N., Ragland, D.A., Rafalowski, M.B., Collins, K., Tsegay, T., McConnell, D., Marchini, D., Beauchamp, W., and Sanderson, D.J., 1986, Geologic highlights in the Blue Creek Canyon area, *in* Donovan, R.N., ed., *The Slick Hills of Southwestern Oklahoma – Fragments of an Aulacogen?: Oklahoma Geological Survey Guidebook 24*, p. 84-91.
- Donovan, R.N., Ragland, D., Cloyd, K., Bridges, S., and Denison, R.E., 1988a, Carlton Rhyolite and lower Paleozoic sedimentary rocks at Bally Mountain in the Slick Hills of southwestern Oklahoma: Geological Society of America Centennial Field Guide—South-Central Section, p. 93-98.
- Donovan, R.N., Younger, P., and Ditzell, C., 1988b, Some aspects of the geology of Zodletone Mountain, southwestern Oklahoma: Geological Society of America Centennial Field Guide—South-Central Section, p. 99-102.
- Frazier, S.J., Hanson, R.E., and McCleery, D.A., 2012, Cambrian volcanic stratigraphy and rhyolite peperite in the Bally Mountain area, SW Oklahoma: Geological Society of America Abstracts with Programs, v. 44, no. 1, p. 7.
- Ham, W.E., Denison, R.E., and Merritt, C.A., 1964, Basement Rocks and Structural Evolution of Southern Oklahoma: Oklahoma Geological Survey Bulletin 95, 302 p.
- Hanson, R.E., and Hargrove, U.S., 1999, Processes of magma/wet-sediment interaction in a large-scale Jurassic andesitic peperite complex, northern Sierra Nevada, California: Bulletin of Volcanology, v. 60, p. 610-626.
- Hanson, R.E., McCleery, D.A., Crowley, J.L., Bowring, S.A., Burkholder, B.K., Finegan, S.A., Philips, C.M., and Pollard, J.B., 2009, Large-scale Cambrian rhyolitic volcanism in southern Oklahoma related to opening of Iapetus: Geological Society of America Abstracts with Programs, v. 41, no. 2, p. 14.
- Hanson, R.E., Puckett, R.E., Jr., Keller, G.R., Brueseke, M.E., Bulen, C.L., Mertzman, S.A., Finegan, S.A., and McCleery, D.A., 2013, Intraplate magmatism related to opening of the southern Iapetus Ocean: Cambrian Wichita igneous province in the Southern Oklahoma rift zone: Lithos, v. 174, p. 57-70.
- Harlton, B.H., 1963, Frontal Wichita Fault System of southwestern Oklahoma: American Association of Petroleum Geologists Bulletin, v. 47, p. 1552-1580.
- Hughes, C.J., 1972, Spilites, keratophyres, and the igneous spectrum: Geological Magazine, v. 109, p. 513-527.
- Kokelaar, B.P., 1982, Fluidization of wet sediments during the emplacement and cooling of various igneous bodies: Geological Society of London Journal, v. 139, p. 21-33.
- McArthur, A.N., Cas, R.A.F., and Orton, G.J., 1998, Distribution and significance of crystalline, perlitic and vesicular textures in the Ordovician Garth Tuff (Wales): Bulletin of Volcanology, v. 60, p. 260-285.
- McCall, R.L., 1994, Structural geology of the Blue Creek Canyon Fault Zone, Slick Hills, southwestern Oklahoma [M.S. thesis]: Fort Worth, Texas, Texas Christian University, 73 p.
- McConnell, D.A., 1989, Determination of offset across the northern margin of the Wichita Uplift, southwest Oklahoma: Geological Society of American Bulletin, v. 101, p. 1317-1332.
- Miller, G.W., and Stanley, T.M., 2004, Geologic Map of the Anadarko 30' X 60' Quadrangle, Caddo, Canadian, Custer, Grady, Kiowa, and Washita Counties, Oklahoma: Oklahoma Geological Survey Map OGQ-58, scale 1:100,000.
- Pearce, J.A., Harris, N.B.W., and Tindle, A.G., 1984, Trace-element discrimination diagrams for the tectonic interpretation of granitic rocks: Journal of Petrology, v. 25, p. 956-983.
- Philips, C.M., 2002, Paleovolcanology of the A-type Carlton Rhyolite, Blue Creek Canyon area, Wichita Mountains, southern Oklahoma [M.S. thesis]: Fort Worth, Texas Christian University, 86 p.
- Powell, B.N., Gilbert, M.C., and Fischer, J.F., 1980, Lithostratigraphic classification of basement rocks of the Wichita Province, Oklahoma: Geological Society of America Bulletin, v. 91, Part I, Summary, p. 509-514; Part II, p. 1875-1994.
- Price, J.D., 1998, Petrology of the Mount Scott Granite [Ph.D. thesis]: Norman, Oklahoma, University of Oklahoma, 240 p.
- Ross, C.S., and Smith, R.L., 1961, Ash-Flow Tuffs: Their Origin, Geologic Relations, and Identification: U.S. Geological Survey Professional Paper 366, 81 p.
- Seaman, S.J., Dyar, M.D., and Marinkovic, N., 2009, The effects of heterogeneity in magma water concentration on the development of flow banding and spherulites in rhyolitic lava: Journal of Volcanology and Geothermal Research, v. 183, p. 157-169.
- Skilling, I.P., White, J.D.L., and McPhie, J., 2002, Peperite: A review of magma-sediment mingling: Journal of Volcanology and Geothermal Research, v. 114, p. 1-17.
- Stanley, T.M., and Miller, G.W., 2005, Geologic Map of the Lawton 30' X 60' Quadrangle, Caddo, Comanche, Grady, Kiowa, Stephens, and Tillman Counties, Oklahoma: Oklahoma Geological Survey Map OGQ-63, scale 1:100,000.
- Sun, S.S., and McDonough, W.F., 1989, Chemical and isotopic systematics of oceanic basalts: Implications for mantle composition and process, *in* Saunders, A.D., and Norry M.J., eds., *Magmatism in the Ocean Basins*: Geological Society of London Special Publications, v. 42, p. 313-345.
- Swanson, S.E., Naney, M.T., Westrich, H.R., and Eichelberger, J.C., 1989, Crystallization history of Obsidian Dome, Inyo Domes, California: Bulletin of Volcanology, v. 51, p. 161-176.
- Whalen, J.B., Currie, K.L., and Chappell, B.W., 1987, A-type granites: Geochemical characteristics, discrimination and petrogenesis: Contributions to Mineralogy and Petrology, v. 95, p. 407-419.
- Winchester, J.A., and Floyd, P.A., 1977, Geochemical discrimination of different magma series and their differentiation products using immobile elements: Chemical Geology, v. 20, p. 325-343.

## **APPENDIX: DESCRIPTIONS OF INDIVIDUAL FLOWS**

### **Blue Creek Canyon**

#### **Flow 1 (>50 m thick)**

*Top of flow:* Locally shows broad undulations on scale of several meters, representing either pressure ridges or relatively large flow folds. Where best exposed, upper 2 m consists of glass altered to green clay with small vesicles also filled with green clay; this passes down into zone several meters thick containing larger, abundant vesicles partly or completely filled with green clay or quartz. Flow lamination is present in uppermost part of flow with variable, locally vertical dips due to flow folding.

*Flow interior:* One or more discontinuous, lithophysal zones locally occur below chilled top of flow and pass into homogeneous to flow-banded and flow-folded, more fel-

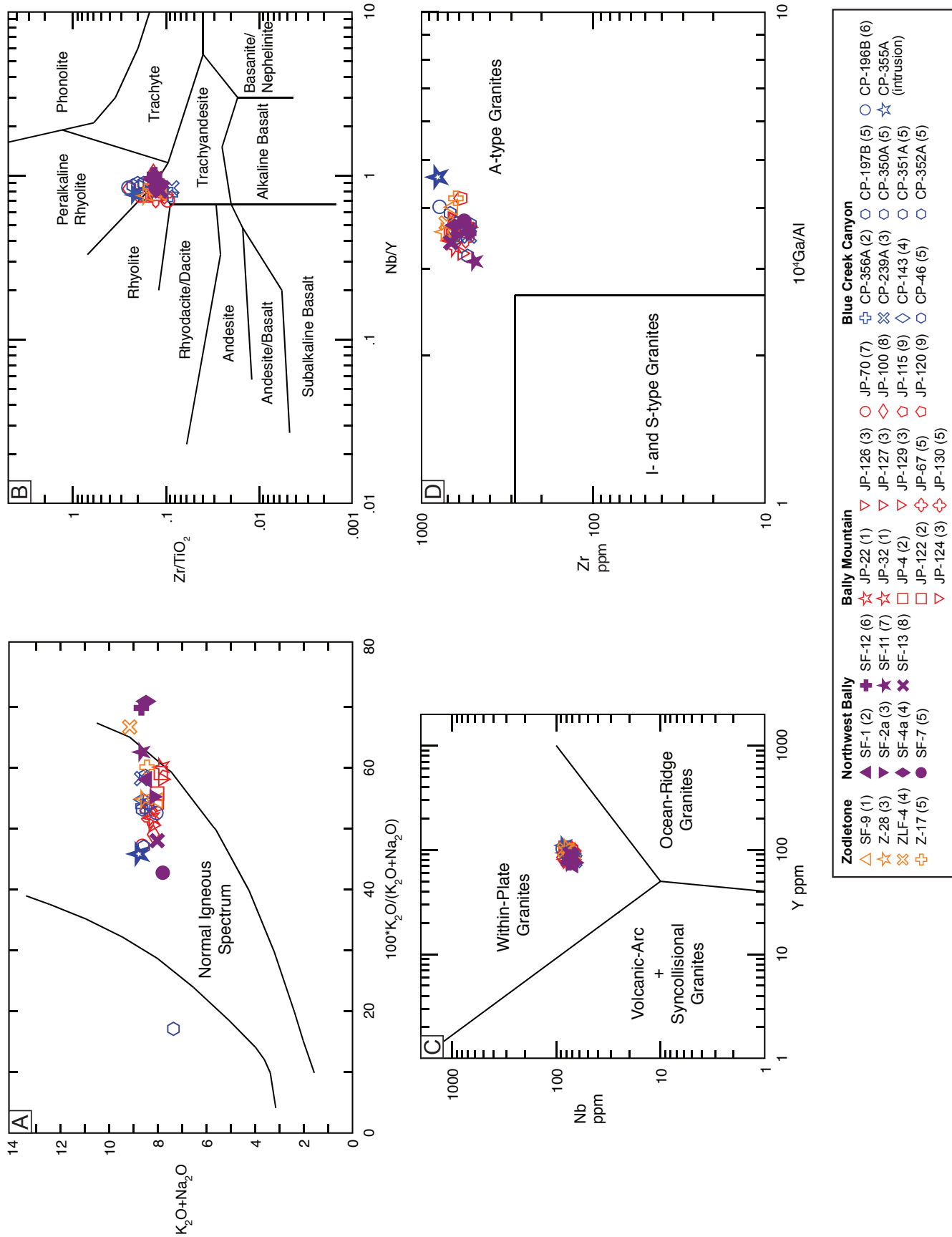
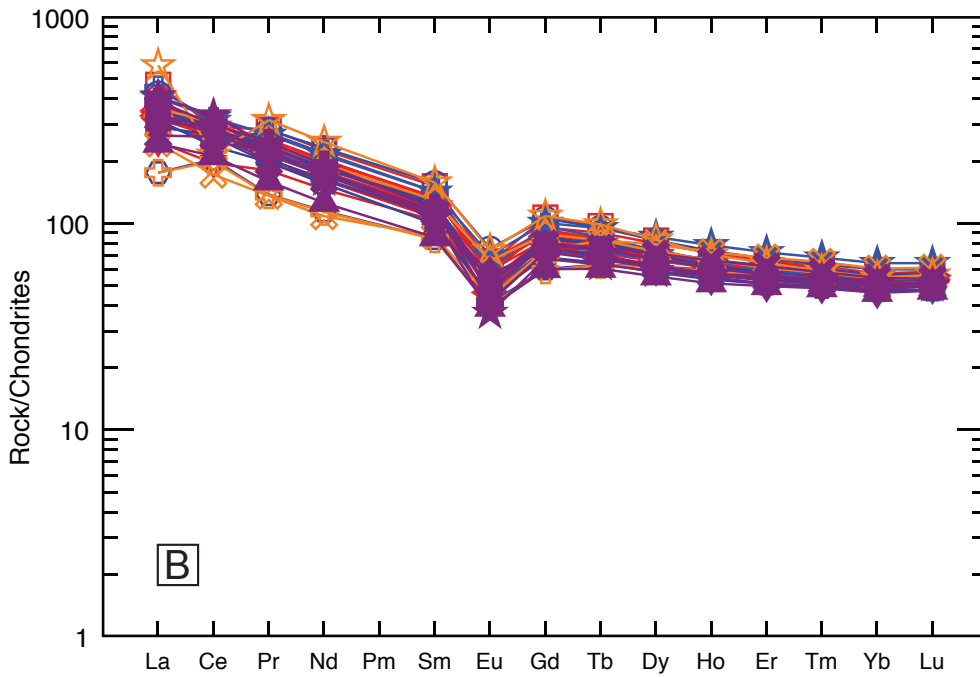
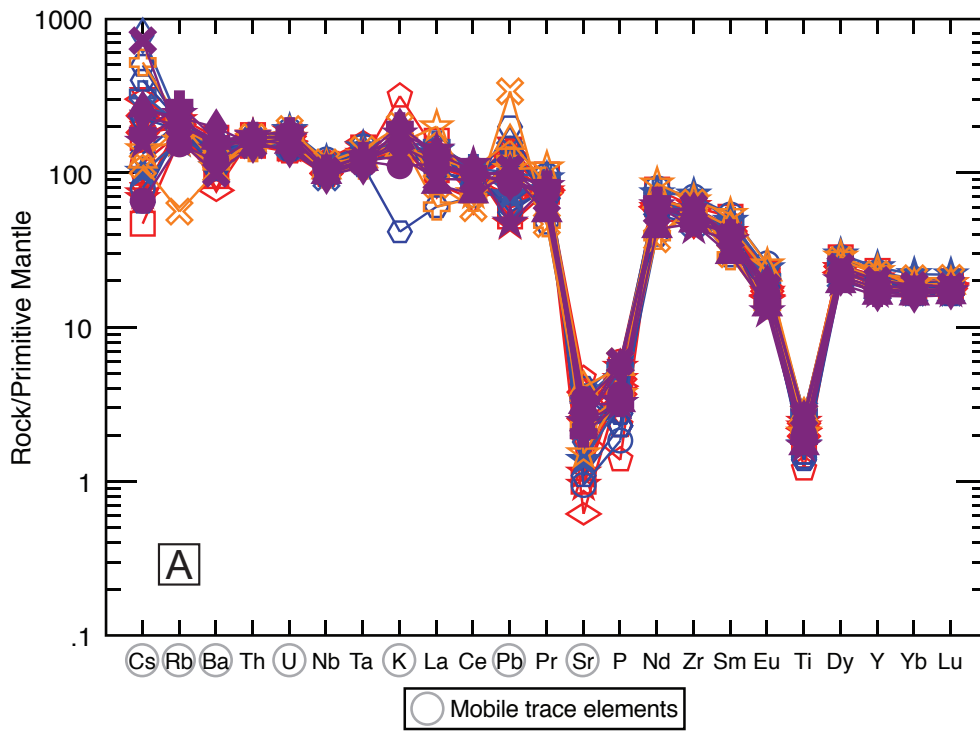


Figure 20. Data for the Carlton Rhyolite in the Slick Hills plotted on selected diagrams. (A) Igneous spectrum diagram of Hughes (1972). (B) Discrimination diagram of Winchester and Floyd (1977). (C) Nb versus Y discrimination diagram of Pearce et al. (1984). (D) Zr versus  $10^4 Ga/Al$  discrimination diagram of Whalen et al. (1987).



Zodletone	Northwest Bally	Bally Mountain	Blue Creek Canyon
△ SF-9 (1)	▲ SF-1 (2)	✦ SF-12 (6)	☆ JP-22 (1)
☆ Z-28 (3)	▼ SF-2a (3)	★ SF-11 (7)	☆ JP-32 (1)
⊗ ZLF-4 (4)	◆ SF-4a (4)	✖ SF-13 (8)	□ JP-4 (2)
⊕ Z-17 (5)	● SF-7 (5)	▽ JP-122 (2)	⊕ JP-67 (5)
		▽ JP-124 (3)	⊕ JP-130 (5)
		▽ JP-126 (3)	○ JP-70 (7)
		▽ JP-127 (3)	◇ JP-100 (8)
		▽ JP-129 (3)	◇ JP-115 (9)
		◇ JP-120 (9)	◇ CP-143 (4)
			◇ CP-46 (5)
			◇ CP-356A (2)
			◇ CP-197B (5)
			◇ CP-196B (6)
			⊗ CP-239A (3)
			◇ CP-350A (5)
			☆ CP-355A (intrusion)
			◇ CP-351A (5)
			◇ CP-352A (5)

Figure 21. Multi-element diagram (A) and REE diagram (B) for the Carlton Rhyolite in the Slick Hills. Normalization values in both diagrams are from Sun and McDonough (1989).

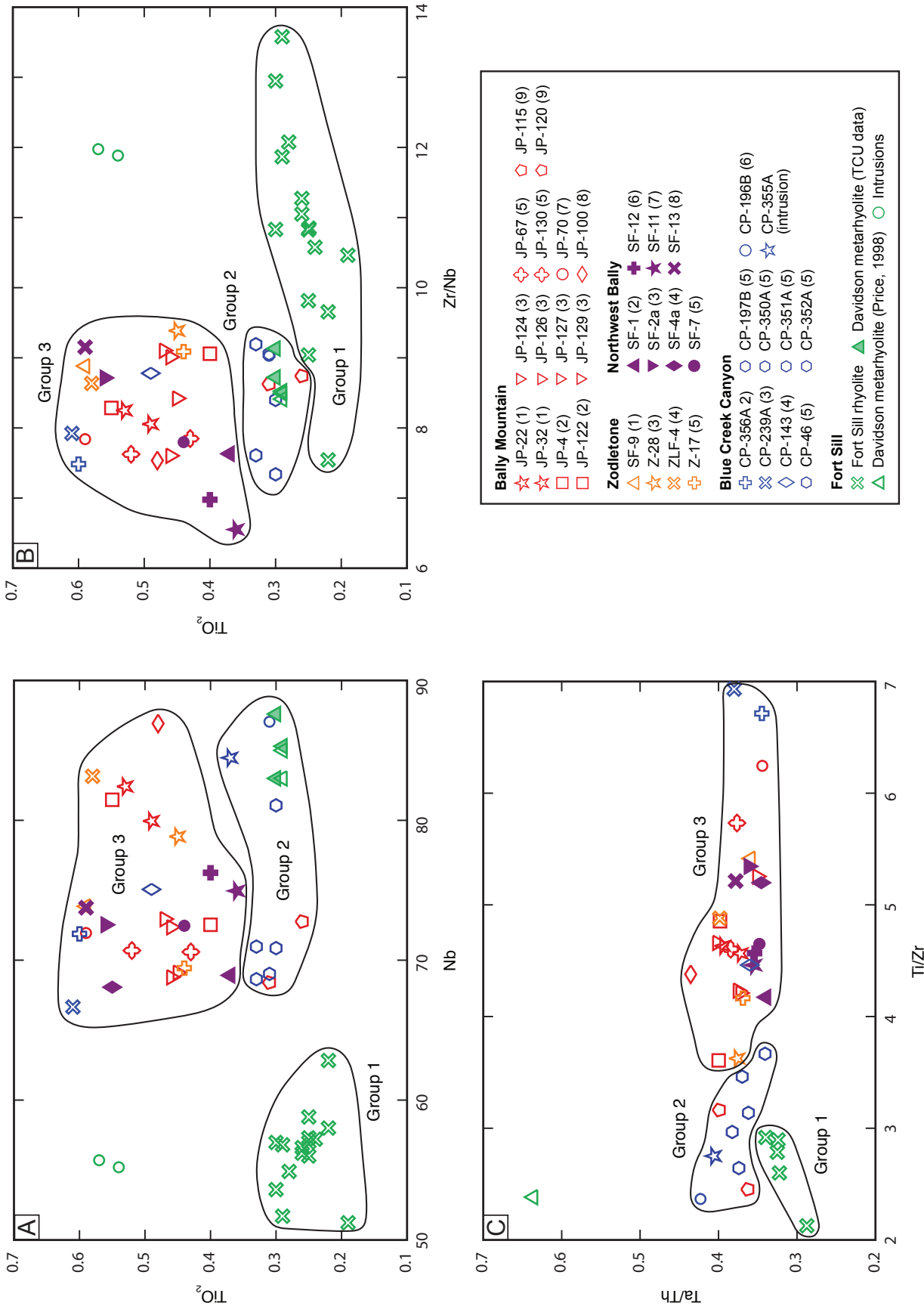


Figure 22. Trace-element diagrams showing distinct groups in the Carlton Rhyolite in the Wichita Mountains. (A)  $TiO_2$  versus Nb diagram. (B)  $TiO_2$  versus Zr/Nb diagram. (C) Ta/Th versus Ti/Zr diagram. Data for the Davidson metarhyolite, Fort Sill rhyolite, and hypabyssal intrusions in the Fort Sill area are from Finegan and Hanson (this guidebook).

sitic, ledge-forming rhyolite, still with common green clay. Flow breccia is present in zones up to several meters thick at different levels in flow. Crude columnar jointing occurs locally. Lower exposed parts of flow show flow banding, flow folding and abundant perlitic texture in altered, green to yellow-brown groundmass; perlitic texture is also present in places higher within flow.

*Base of flow:* Covered, but southernmost outcrops are probably close to flow base because of abundance of perlitic.

#### **Flow 2 (230 m thick)**

*Top of flow:* Near top, groundmass has altered appearance and dark-green to yellow-gray or brown color. Small quartz-filled vesicles are present in places as well as abundant flow banding and lamination, with flow folding and local flow breccia.

*Flow interior:* Lithophysae as much as 2.5 cm across are present below chilled upper margin in zone up to 5.5 m thick. Lithophysae (in some cases as much as 18 cm across) also occur above chilled base of flow and are concentrated in layers parallel to flow banding. Lithophysal zones pass inward into felsitic flow interior that typically shows flow banding with columnar and/or sheeting joints present in places.

*Base of flow:* Peperite is exposed in several places along base and locally passes up into flow breccia lacking interstitial sediment; in some other places, flow breccia is present near or along lower contact without peperite. Same altered appearance to groundmass as at flow top, with common perlitic texture. Irregular, flow-aligned, partly quartz-filled vesicles occur locally. Flow banding and lamination are approximately parallel to flow base where not affected by strong flow folding.

#### **Flow 3 (170 m thick)**

*Top of flow:* Green to brown, altered glassy groundmass with abundant small vesicles in some layers. Flow breccia is exposed at numerous places near or at flow top; elsewhere, flow banding/lamination is typically subparallel to contact where not affected by flow folding.

*Flow interior:* Altered, glassy zones along top and base of flow grade inward to felsitic flow interior that shows columnar joints perpendicular to flow base; prominent sheeting joints also occur in places, forming tombstone topography. Flow banding occurs in lower and upper parts of felsitic zone. Lithophysae as much as 5 cm across appear several meters below top and in places form a distinct zone as much as 30 m thick in upper part of flow interior. In contrast, lithophysae occur only rarely near flow base.

*Base of flow:* Slope-forming, dark-green to brown, altered glassy groundmass showing perlitic texture and flow banding/lamination, with quartz-lined vesicles a few millimeters long. Relict pumice is present in a few outcrops near or at base. Altered, glassy basal zone becomes thicker in western exposed part of flow where it comprises about one third of the total flow thickness. Flow breccia is discontinuous but forms numerous outcrops all along exposed base of flow and passes downward and laterally into peperite. Breccia typically grades upward into flow-banded lava. Where breccia is absent, flow lamination is commonly exposed along flow base and in some cases is deformed by small flow folds.

#### **Flow 4 (200 m thick)**

*Top of flow:* Brown to dark-green groundmass, strongly perlitic in places, with columnar jointing. Flow banding/lamination shows flow lineation and open to tight or isoclinal flow folding in places. Flow breccia is also locally present near or at top.

*Flow interior:* Below upper chilled margin, lithophysae as much as 4 cm across are locally abundant in a zone ~3.4 m thick within flow-banded and flow-folded lava. Groundmass becomes felsitic in flow interior and shows crude columns 1.5 m across; sheeting joints are also present and locally form two different sets at a high angle to each other. Flow banding is present in places all the way into flow center.

*Base of flow:* Slope-forming, altered green groundmass showing flow banding/lamination. Lithophysae are locally present very close to base. Peperite is locally present along flow base and in some cases passes up into flow breccia lacking sediment between rhyolite clasts.

#### **Flow 5 (200 m thick)**

*Top of flow:* Dark-green to brown groundmass with perlitic texture locally occurs in zone  $\geq 4.5$  m thick at top of flow and forms recessive outcrops; this in places shows flow banding or delicate flow lamination defined by green and pink-gray layers and elsewhere appears massive in hand sample. Flow lineation and flow folds also occur, and some small, isoclinal flow folds show an axial planar fabric. Very abundant, small irregular vesicles, partly to completely filled with chlorite or quartz, are aligned in flow direction. Flow breccia crops out in one place at flow top.

*Flow interior:* Interior is felsitic, with common ledge-forming outcrops showing columnar jointing and generally consistently northeast-dipping flow banding. Downslope from chilled upper margin lithophysae as much as 4 cm across begin to appear and are abundant in places

in distinct zone above felsitic interior. Chilled lower margin grades into felsitic interior ~4.5 m above flow base; thin zone rich in lithophysae  $\leq 1.2$  cm in diameter occurs below transition into felsite.

*Base of flow:* Groundmass tends to have brown or dark-purple color with altered appearance. Flow banding and lamination typically dip northeast, roughly parallel to flow base, and in some cases show flow lineation. Columnar jointing is well developed in places; columns extend to flow base and are perpendicular to it. Basal flow breccia is locally present and flow banding in other places shows incipient brecciation. Elsewhere flow-laminated base is in sharp contact with flow 4 or rests directly on thin tuffaceous interbed between flows. Lithophysae as much as 1.2 cm across are locally present close to base.

**Flow 6** (>100 m thick; upper part of flow has been removed by erosion along unconformity with overlying sedimentary strata)

*Flow interior:* Groundmass typically has felsitic texture with very fine grained, granular texture under hand lens. Generally consistently northwest-dipping flow banding or lamination is present where not affected by flow folds, and flow lineation is present in places. Sheeting joints are developed parallel to flow banding in places but in other cases have much steeper dips and cut across banding. Flow folds typically are open with wavelengths as much as a few meters. Crude but locally pervasive columnar jointing is perpendicular to base of flow. Western outcrops in places show flow banding and lamination with local flow folding and columnar jointing, but these outcrops are typically strongly altered due to proximity to faults.

*Base of flow:* Base of flow is locally well exposed and rests directly on top of flow 5 with no intervening sediment. In places the base is defined by a distinct ledge of partly perlitic flow-laminated lava a few meters thick with lithophysae as much as 30 cm across; columnar jointing is perpendicular to flow lamination and flow base. Elsewhere lowest part of flow consists of flow-laminated, less well-exposed rhyolite with dark-brown altered groundmass with perlitic texture.

**Flow 7** (>25 m thick; most of the flow has probably been removed by erosion along the unconformity)

*Base of flow:* Altered groundmass, with flow banding and flow folding.

## Bally Mountain

**Flow 1** (>280 m thick)

*Top of flow:* Covered; flow is only exposed in two small hills.

*Flow interior:* Western outcrop shows pervasive flow banding and millimeter-scale lamination with well-developed flow lineation visible in places; minor flow breccia is present. Flow banding wraps a fluidal basaltic inclusion 2.5 cm long. In eastern outcrop, banding remains pervasive but lacks flow lineation. Flow banding is deformed by open to tight, meter-scale flow folds with rounded hinges, and columnar joints cut flow banding at a high angle in both outcrops. Planar sheeting joints in places follow flow banding, and in other places curved sheeting joints cut the banding. Groundmass in western outcrop has a heterogeneous appearance, with patches of orange-gray to dark purple-gray visible under hand lens. Eastern outcrop has more uniform, felsitic, red-brown groundmass.

*Base of flow:* Western outcrop is probably near flow base because of prominence of flow lamination and more heterogeneous appearance to groundmass.

**Flow 2** (>100 m thick)

*Top of flow:* Upper part of flow consists largely of clast-supported flow breccia as much as 40 m thick with angular clasts generally ranging from <1 cm to ~1 m across; many clasts show internal flow banding or lamination and flow folding truncated by clast margins and rotated relative to adjacent clasts. Clasts are typically felsitic, but dark gray-green perlitic clasts are locally present near top of breccia. Uppermost part of flow breccia is infiltrated by tuffaceous material where overlying bedded tuffaceous rocks are preserved; elsewhere breccia is in direct contact with peperite developed at base of overlying flow. In lower part of breccia a large raft of flow-banded lava as much as 2.4 m thick and  $\leq 6$  m long grades on all sides into breccia. Other smaller clasts in breccia also show progressive disruption along their margins.

*Flow interior:* Flow breccia is underlain by felsitic, brown-red rhyolite, in places with prominent sheeting joints sub-parallel to overall dip of rhyolite succession in Bally Mountain area. In other outcrops, flow banding is present and is deformed by generally upright flow folds with wavelengths of as much as several meters. Sparse basaltic inclusions as much as 2.5 cm long are present. Contact with flow breccia is gradational, with patches and lenses of breccia progressively developing upward in flow-banded

rhyolite until outcrop is dominated by breccia. Crude columns are locally present.

*Base of flow:* Covered.

**Flow 3** (370 m thick)

*Top of flow:* Uppermost part of flow, in direct contact with overlying lava flow, shows thin, prominent flow lamination defined by alternating pink and green layers and affected by flow folding. Lithophysae 2.5 to 8 cm across make as much as ~25% of upper 13 m of flow and cut across flow banding. Much of the groundmass outside the lithophysae is rich in green clay.

*Flow interior:* Main part of flow is homogeneous, unbanding felsite. Columns typically from 30 cm to 1.5 m across are perpendicular to flow base and top and occur in lower and upper parts of flow. Sheeting joints are present throughout most of flow and are commonly parallel to the flow base in lower part of flow above basal flow-banded zone. Higher up, vertical sheeting joints are present in places, and much of flow interior shows curvilinear sheeting joints, in some cases forming multiple intersecting sets. The curvilinear sheeting joints pass abruptly upward into a zone of flow parting parallel to flow top.

*Base of flow:* Locally in direct contact with undisturbed, bedded volcanoclastic rocks, but well-developed peperite is generally present (see text). Flow banding or lamination is typically present in a zone as much as several meters thick in lower part of flow, parallel to flow base, and locally shows open flow folding.

**Flow 4** (>30 m thick)

*Top of flow:* Missing; overlying volcanoclastic rocks occupy a channel cut into flow.

*Flow interior:* May have been largely eroded away prior to deposition of overlying volcanoclastic rocks. Upper preserved part of flow develops a finely mottled greenish to pinkish groundmass in hand sample, with delicate flow lamination but without visible perlitic texture. Flow lamination is nearly vertical at contact against overlying volcanoclastic rocks.

*Base of flow:* Groundmass in lower part of flow has a distinctive dark brown-gray to greenish-black color with perlitic texture readily apparent in hand sample. Flow breccia is developed in places.

**Flow 5** (125 m thick)

*Top of flow:* Flow banding parallel to flow top is developed in upper part of flow. A prominent lithophysal zone makes up the upper 5 m of the flow. The lithophysae

cut across flow banding and increase in size upward from ~1 cm across to as much as 2.5 cm. They also increase in abundance upward, comprising most of rock in a zone ~1 m thick at the flow top; this zone is laterally persistent on the scale of the available outcrop.

*Flow interior:* Flow lamination disappears upward from base within central zone of homogeneous felsitic rhyolite, with generally consistent, thinly spaced sheeting joints or flow parting parallel to base of flow.

*Base of flow:* Peperite is developed at base of flow against underlying planar-laminated vitric tuff. Above peperite, lower 2 m of flow has dark-green groundmass with delicate flow lamination that shows flow folding in places.

**Flow 6** (90 m thick)

*Top of flow:* Felsitic interior passes up into zone of pervasive flow banding; bands are ~1 to 3 cm thick, with dark-green, originally glassy layers alternating with pink-gray or orange-gray spherulitic layers. Banding within 2 m of base of overlying flow develops steep dips in places due to flow folding; actual flow top is covered.

*Flow interior:* Green groundmass in lower 15 m of flow grades upward into pinkish-brown felsitic rhyolite in flow interior. Flow parting is present, and relatively crude, pseudohexagonal columnar joints are perpendicular to flow parting.

*Base of flow:* Lowest outcrops of flow are separated by <1 m of cover from top of flow 5 and have green groundmass representing altered glass. Peperite crops out in a few places along base; sediment host to rhyolite clasts in the peperite is very fine grained siliceous tuff. No intact tuff interbed was observed below the flow but could be covered. Abundant irregular vesicles <1 mm long and filled with microcrystalline quartz form a distinct zone in basal 2 m of flow. Green groundmass is present in lower 15 m of flow, and flow banding defined by pink to dark-green bands and deformed by centimeter- to meter-scale flow folds occurs in parts of this interval.

**Flow 7** (>40 m thick)

*Top of flow:* Covered.

*Flow interior:* Lower part of flow passes into zone of abundant flow banding defined by pink-gray more resistant layers as much as 2.5 cm thick alternating with thinner, darker, more easily weathered layers. Lithophysae as much as 8 cm across are abundant. Flow bands show complex centimeter- to meter-scale flow folds and refolded folds in places; sheath folds are also present. Limbs of some folds

are sheared off parallel to flow banding. Closely spaced fractures cross the flow banding and in some cases are axial planar to flow folds. The zone of abundant flow banding passes abruptly upward 19 m above flow base into a more homogeneous felsitic zone which shows some flow banding, but not as well developed as below. This interval is characterized by flow parting or sheeting joints parallel to regional dip, with columnar joints perpendicular to parting. Along strike to the northwest the felsitic rhyolite crops out within 2 m of the flow base, which is covered, suggesting that the lower zone of green, altered glass and the overlying zone of well-developed flow banding are locally thin or absent.

*Base of flow:* Much of lower 8 m of flow has homogeneous green groundmass representing altered glass, but flow banding defined by layers of pink-gray or orange-gray felsitic or spherulitic rhyolite alternating with green, altered glass occurs in places in this interval, along with some lithophysae.

#### **Flow 8 (>100 m thick)**

*Top of flow:* In upper few meters, delicate flow banding parallel to flow top develops, with locally abundant lithophysae as much as 2 cm across.

*Flow interior:* Typical orange-gray felsite, with columnar joints perpendicular to flow top crossed by sheeting joints.

*Base of flow:* Covered.

#### **Flow 9 (>130 m thick)**

*Top of flow:* Erosional top is unconformity with Reagan Sandstone, with a paleohill rising above the general surface of the unconformity along the northwest exposed part of the contact. Away from the paleohill, the rhyolite shows thin, well-developed flow banding that generally dips consistently northeast and shows a small angular discordance with bedding in the overlying Reagan strata. Flow banding locally shows flow folding and grades in places into patches of flow breccia  $\leq 20$  cm across. At higher levels in the flow, which are exposed in the paleohill, the flow banding becomes pervasive with individual bands typically  $\leq 1$  cm across and well-developed flow lineation commonly parallel to axes of early flow folds, which are commonly refolded. The well-developed flow banding and abundant flow folds suggest that this part of the flow is close to the original top.

*Flow interior:* Lower glassy zone passes up into a laterally continuous, ledge-forming interval 1.2 m thick with well-defined flow banding and lamination deformed by re-

cumbent isoclinal flow folds; folds show an axial planar fabric defined by spaced shear fractures. The flow banding becomes less well developed upward as the felsitic interior of the flow is approached. Prominent flow parting parallel to the banding is present in places and is cut at right angles by columnar joints.

*Base of flow:* Contact with flow below is covered but can be located within  $\sim 1$  m. Lower part of flow consists of an originally glassy zone with perlitic texture and pumiceous texture in places. The pumiceous rhyolite is mixed on a small scale with disaggregated siliceous vitric tuff, forming peperite (see text for a more thorough discussion of this interval).

### **Northwest Bally Mountain**

#### **Flow 1 (>60 m thick)**

*Top of flow:* Top is covered, but upper exposed part of flow shows well-developed flow banding warped by broad, gentle flow folds. Locally passes up into flow breccia.

*Flow interior:* Groundmass is somewhat felsitic and dark purple-red. Flow banding and lamination from a few millimeters to 2.5 cm thick are visible in places and have variable attitudes due to flow folding. Columns  $\sim 1$  m across are crossed at right angles by well-developed sheeting joints which are probably parallel to flow base. Both columns and sheeting joints cut across the flow banding and lamination in places.

*Base of flow:* Covered.

#### **Flow 2 (>30 m thick)**

*Top of flow:* Pervasive flow banding and millimeter-scale flow lamination in upper part of flow generally dip subparallel to flow top and grade into areas of flow breccia as much as 15 cm across. Banding and lamination are defined by pink and green layers deformed by isoclinal flow folds with wavelengths of  $\sim 60$  cm and are also warped by gently plunging open folds with wavelengths of  $\sim 2$  m. Sparse lithophysae 4 cm across are present and cut across flow lamination. Groundmass develops a dark-green color near top of flow, representing altered glass, and contains small vesicles lined in places with cristobalite crystals (inverted to quartz) visible in thin section.

*Flow interior:* Sheeting joints are developed parallel to flow banding or cut across it where flow folds are present. Crude columnar jointing is visible in places and is approximately perpendicular to flow top.

*Base of flow:* Covered.

**Flow 3** (>45 m thick)

*Top of flow:* Thin zone of flow breccia is exposed in uppermost outcrops of flow, suggesting these outcrops are near the covered top of the flow.

*Flow interior:* Pervasive flow banding and flow lamination dip significantly more steeply than general attitude of lavas in this area. Sheeting joints appear in upper exposed parts of flow. Flow lamination in places shows complex, disharmonic small-scale flow folds that grade into flow breccia toward base of flow. Groundmass contains very fine grained yellow-gray spherulites in a darker groundmass, and lithophysae as much as 5 cm across are locally present.

*Base of flow:* Peperite occurs in a narrow zone at flow base and represents a thin, completely disrupted interbed of dark-brown tuffaceous mudstone, siltstone, and tuff. Sediment within the peperite forms irregular small patches and fills fractures separating angular to fluidal, red-brown perlitic rhyolite fragments as much as several centimeters in length. Rhyolite within and above the peperite contains elongate amygdules <1 mm long filled with quartz and green clay. Flow breccia lacking a sediment matrix between rhyolite clasts locally occurs above the peperite.

**Flow 4** (>70 m thick)

*Top of flow:* Unbanded felsite in flow interior grades up into flow-banded and flow-laminated lava with alternating pink and green layers. Attitude of banding in some places is similar to that of flow banding below felsitic interior, but elsewhere banding in upper part of flow develops steep dips and grades into flow breccia near flow top.

*Flow interior:* Massive, ledge-forming, homogeneous pink-gray felsite several meters thick separates the flow into lower and upper flow-banded zones. Crude columnar jointing perpendicular to flow base is present both in the felsitic interior and in the flow-banded zones.

*Base of flow:* Actual base is covered, but lowest outcrops have a dark gray-green groundmass representing altered glass, which suggests proximity to flow base. Pervasive flow banding with consistent attitudes subparallel to flow base appears a few meters higher in the flow but passes upward into narrow zone of unbanded felsite in flow interior.

**Flow 5** (>70 m thick)

*Top of flow:* Covered.

*Flow interior:* A ledge-forming zone of felsite that can be traced discontinuously along strike a short distance above the basal flow-banded lava develops pervasive,

thinly spaced ( $\leq 1$  cm), locally curvilinear sheeting joints. Higher in the flow the groundmass is uniformly gray-green and sheeting joints are absent. An ovoid-shaped area showing well-developed columnar jointing occurs at this level in one part of the flow. The columns are only 20 to 30 cm across, making them significantly thinner than in most other examples of columnar jointing in Carlton Rhyolite flows, and have an anomalous plunge to the northeast. The rhyolite in the columnar-jointed domain is lithologically identical to that in other parts of the flow at this level, and there is no evidence that it is a later intrusion.

*Base of flow:* Basal flow breccia occurs locally above bedded volcanoclastic interval beneath flow but shows no evidence for peperite, although exposure is poor. Elsewhere, rhyolite at the base has a sharp, planar contact against the underlying volcanoclastic beds. Delicate flow lamination parallel to the contact is deformed in places by small-scale recumbent isoclinal flow folds. Rhyolite is dark gray-green with perlitic texture or has a finely mottled, yellow-gray to red-brown appearance due to heterogeneous development of small-scale devitrification domains.

**Flow 6** (>35 m thick)

*Top of flow:* Flow breccia is visible in places along top, passing down into flow-banded lava containing abundant lithophysae as much as 4 cm across.

*Flow interior:* Flow-banded upper and lower parts of flow grade inward to ledge-forming felsite with pervasive sheeting joints.

*Base of flow:* Covered, but a few meters of flow breccia is locally present in the lowest exposed part of the flow. Flow breccia passes up into zone of well-developed flow banding with abundant lithophysae.

**Flow 7** (>30 m)

*Top of flow:* Covered.

*Flow interior:* Flow breccia passes up into flow-banded zone with a delicate, sub-millimeter-scale flow lamination visible on fresh surfaces. Lithophysae are present in places. Banding shows varying dips due to flow folding and is cut by columnar jointing perpendicular to flow base.

*Base of flow:* Peperite as much as 20 cm thick is locally exposed along base and contains rhyolite clasts mixed with very fine grained, light-gray siliceous tuff, although no intact tuff is preserved. Peperite is overlain by a zone of well-developed flow breccia containing angular to subangular rhyolite clasts  $\leq 15$  cm across without any intermixed sediment.

**Flow 8** (>40 m thick)

*Top of flow:* Covered.

*Flow interior:* Lowest exposed part of flow contains small vesicles filled with quartz and shows flow banding and flow lamination deformed by flow folds with fold interference patterns. Slightly higher, banding shows more uniform attitude approximately parallel to general layering in rhyolite succession and is crossed by columnar joints. The flow-banded zone passes up into the felsitic interior of the flow which shows sheeting joints. This, in turn, passes up into a zone of flow banding with pronounced flow lineation.

*Base of flow:* Covered.

**Zodletone Mountain**

**Flow 1** (>75 m thick)

*Top of flow:* Covered.

*Flow interior:* Flow lamination with consistent north-west dips is pervasively developed throughout entire exposed thickness of flow and is crossed by well-developed columnar jointing perpendicular to flow base.

*Flow base:* Covered, but lowest outcrops are gray-green on fresh surfaces with perlitic texture visible in hand sample, suggesting these outcrops are near flow base. Pervasive flow lamination is present.

**Flow 2** (>40 m thick)

*Top of flow:* Most of exposed part of flow consists of upper flow-banded zone ~15 m thick containing abundant lithophysae 1.2 to 4 cm across, coalescing in places.

*Flow interior:* Upper flow-banded zone passes downward into rhyolite with less well defined flow banding and finely spherulitic groundmass, which is inferred to represent start of flow interior. Lithophysae are absent. Sheeting joints are parallel to flow banding and are cut by columnar joints defining columns 1.0 to 1.5 m wide. Only about 5 m of the flow interior are exposed.

*Flow base:* Covered, along with an unknown thickness of the flow interior.

**Flow 3** (230 m thick)

*Top of flow:* Upper part of flow exhibits well-developed flow banding with spherulites concentrated in some bands.

*Flow interior:* Flow breccia in lower part of flow passes up into flow-banded rhyolite in which bands are defined by changes in color from gray-green to dark-gray. This is overlain by felsitic rhyolite with sheeting joints generally

dipping northeast and cut at right angles by columnar joints defining columns 0.5 to 1 m across. Faint flow banding defined by color differences is only locally present.

*Base of flow:* Base is defined by zone of flow breccia ~70 m thick containing orange-gray to dark purple-gray rhyolite clasts; the purple-gray rhyolite shows perlitic texture.

**Flow 4** (250 m thick)

*Top of flow:* Flow breccia  $\geq 10$  m thick occurs locally at top of flow and contains massive or flow-laminated angular clasts as much as 25 cm long. The flow breccia pinches out laterally. Where it is absent the uppermost part of the flow shows pervasive flow banding and lamination deformed by flow folds at various scales. Much of the groundmass consists of dark gray-green altered glass with perlitic texture visible in places, as well as millimeter-scale quartz-filled vesicles. Lithophysae as much as 2.5 cm across are abundant in places near or at flow top.

*Flow interior:* Most of the flow interior shows pervasive flow banding and lamination. Thicker flow bands are defined partly by coalescing spherulites, and thinner laminae are defined by variations in color. Flow lineation is present on the surfaces of some laminae. Flow folds with wavelengths of meters to tens of meters are common. Flow breccia and areas where the groundmass has a dark-gray or black color and shows perlitic texture locally occur well within flow interior. Lithophysae as much as 3 cm across occur in places and cut across flow banding. Two distinct areas in the upper part of the flow interior have a more felsitic groundmass and contain well-developed columns that are perpendicular to northerly dipping flow banding. In places the columns are only 10 to 25 cm across, but in other places they are as much as 45 cm across. The larger felsitic area is nearly 100 m across with a roughly elliptical shape and is directly overlain by flow breccia in the upper part of the flow. The smaller felsitic area forms a crudely lenticular mass ~14 m long and 4.5 m high and is encased by a lithophysal zone 5 m thick.

*Base of flow:* At the flow base, which is defined by a distinct saddle in the topography, peperite is locally present with thin, discontinuous lenses or tongues of very fine grained, siliceous vitric tuff contained within rhyolite lava. Some of the tuff lenses preserve planar lamination, and tricuspidate shards are visible with a hand lens. The peperitic zone is overlain by flow breccia ~20 m thick. Another local zone of peperite a few meters across occurs near the top of the zone of flow breccia and consists of angular blocks of rhyolite separated by irregular pockets of the same type

of vitric tuff as is present at flow base. The flow breccia passes up into typical flow-banded rhyolite of flow interior.

**Flow 5 (>190 m thick)**

*Top of flow:* As the flow top is approached from below the felsitic groundmass characteristic of the flow interior begins to develop a finely mottled appearance in shades of pink-gray and gray-green. The top is covered, but local outcrops and large, locally derived pieces of float in this area consist of dark gray-green rhyolite that is interpreted to come from the uppermost part of the flow and contains small vesicles filled with quartz and larger gas cavities as much as 2.5 cm across lined with drusy quartz crystals. The groundmass in places has a gray-green color and shows perlitic texture.

*Flow interior:* Flow-banded and spherulitic zone grades up into felsitic interior which forms prominent, cliffy outcrops. Sheeting joints are also present and are parallel in places to a pervasive flow lamination that becomes progressively less well defined and then disappears higher in the flow interior. Sheeting joints generally dip consistently northeast and are perpendicular to relatively well developed columns 45 cm to 1.5 m across.

*Base of flow:* Base is only well exposed in one area where rhyolite lava rests on fine-grained, altered, crystal-vitric rhyolite tuff that is ~1 m thick and can be traced for ~10 m along strike before becoming covered. Rhyolite just above tuff shows flow lamination parallel to contact. In another area near the base, the lowest exposed parts of the flow consist of several meters of dark-gray, pervasively perlitic, altered glass lacking distinct flow banding. Elsewhere, the lowest exposed parts of the flow show pervasive, centimeter-scale flow parting parallel to flow base and indistinct flow banding defined by color changes. The groundmass consists of yellow-green altered glass with common ovoid to irregular quartz-filled vesicles 1 to 2 mm long and parallel to banding. Slightly higher, the vesicles become more abundant and larger (as much as 1 cm long), and spherulites as much as 0.75 cm across also become abundant. A little higher in the flow, some bands contain numerous white spherulites  $\leq 2$  mm across set within a green groundmass. Columnar jointing is present and defines columns from 20 cm to 2 m across in different areas.

